HHS Public Access

Author manuscript

J Med Chem. Author manuscript; available in PMC 2016 October 22.

Published in final edited form as:

J Med Chem. 2015 October 22; 58(20): 7991–8010. doi:10.1021/acs.jmedchem.5b00805.

Novel 3-Substituted 7-Phenylpyrrolo[3,2-*f*]quinolin-9(6*H*)-ones as Single Entities with Multitarget Antiproliferative Activity

Davide Carta[†,‖], **Roberta Bortolozzi**[‡,‖], **Ernest Hamel**[§], **Giuseppe Basso**[‡], **Stefano Moro**[†], **Giampietro Viola**[‡], and **Maria Grazia Ferlin**[*,†]

[†]Department of Pharmaceutical and Pharmacological Sciences, University of Padova, Via Marzolo, 5, 35131 Padova, Italy

[‡]Laboratory of Oncohematology, Department of Women's and Children's Health, University of Padova, 35128 Padova, Italy

[§]Screening Technologies Branch, Developmental Therapeutics Program, Division of Cancer Treatment and Diagnosis, Frederick National Laboratory for Cancer Research, National Cancer Institute, National Institutes of Health, Frederick, Maryland 21702, United States

Abstract

A series of chemically modified 7-phenylpyrrolo[3,2-*f*] quinolinones was synthesized and evaluated as anticancer agents. Among them, the most cytotoxic (subnanomolar GI_{50} values) amidic derivative **5f** was shown to act as an inhibitor of tubulin polymerization (IC_{50}, 0.99 μM) by binding to the colchicine site with high affinity. Moreover, **5f** induced cell cycle arrest in the G2/M phase of the cell cycle in a concentration dependent manner, followed by caspase-dependent apoptotic cell death. Compound **5f** also showed lower toxicity in nontumoral cells, suggesting selectivity toward cancer cells. Additional experiments revealed that **5f** inhibited the enzymatic activity of multiple kinases, including AURKA, FLT3, GSK3A, MAP3K, MEK, RSK2, RSK4, PLK4, ULK1, and JAK1. Computational studies showed that **5f** can be properly accommodated in the colchicine binding site of tubulin as well as in the ATP binding clefts of all examined kinases. Our data indicate that the excellent antiproliferative profile of **5f** may be derived from its interactions with multiple cellular targets.

[*]**Corresponding Author**mariagrazia.ferlin@unipd.it. Fax: (+39) 0498275366. Phone: (+39) 0498271603..

[‖]D.A. and R.B. contributed equally to this work.

Supporting Information

The Supporting Information is available free of charge on the ACS Publications website at DOI: 10.1021/acs.jmedchem.5b00805. Complete ^{1}H and ^{13}C NMR signals assignment and structure elucidation for compound **10**; ^{1}H NMR spectrum (400 MHz, DMSO-d_6) of compound **10**; $^{13}C\{^{1}H\}$ NMR spectrum (101 MHz, DMSO-d_6) of compound **10**; ^{1}H–^{1}H 2D COSY and ^{1}H–^{13}C 2D HMBC NMR correlation tables (DMSO-d_6) of compound **10**; HRMS (ESI-MS, 140 eV) spectrum of compound **10**; HPLC trace of compound **10**; complete ^{1}H and ^{13}C NMR signals assignment and structure elucidation for compound **18**; ^{1}H NMR spectrum (400 MHz, DMSO-d_6) of compound **18**; $^{13}C\{^{1}H\}$ NMR spectrum (101 MHz, DMSO-d_6) of compound **18**; ^{1}H–^{1}H 2D COSY NMR correlation table (DMSO-d_6) of compound **18**; HRMS (ESI-MS, 140 eV) spectrum of compound **18**; HPLC trace of compound **18**; HRMS (ESI, 140 eV) spectra and HPLC traces of compounds **5a–f**, **8f**, **9**, **11–17**; behavior of compound **18** in aqueous solution at various pH values; elemental analysis of all final compounds **5a–f**, **8f**, and **9–18**; combination cytotoxicity of **5f** and daunorubucine (Dauno), dexamethasone (Dex), cytarabine (Ara-C); dose–response curves of Jurkat (A) and THP1 (B) to **5f**; Table S2 of the collected PDB structures and the corresponding references; Table S3 of simplified molecular-input line-entry for all final compounds **5a–f**, **8f**, and **9–18** (PDF) Molecular formula strings (CSV)

Notes

The authors declare no competing financial interest.

Abstract

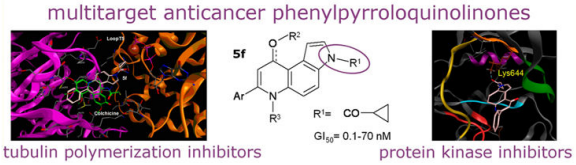

INTRODUCTION

Cancer is a leading cause of disease worldwide, accounting for 12.7 million new cases every year, and this number is expected to rise to 26 million by 2030. Considering the impact on human health and economics, cancer presents a major challenge to the scientific world, and there is a necessity to discover new agents for the treatment of this disease. Most of the drugs in preclinical development are represented by small molecules. In 2013, for example, 9 out of 10 new cancer drugs launched on the market were small molecules.[1]

Currently, combined anticancer therapies or multitargeted drugs are preferred over traditional cytotoxic treatment, with the aim to overcome resistance and toxicity drawbacks. These events often prevent successful treatment and are responsible for reduced survival times.[2] In the field of chemotherapeutics, the widely used antitubulin agents exhibit significant cytotoxicity by inhibiting microtubule dynamics. There are several structurally dissimilar small molecules with high affinity for the colchicine site on tubulin able to inhibit the proliferation of a wide variety of human cancer cells. Moreover, these agents also affect the tumor endothelial vasculature required for the growth of tumor mass. These types of tubulin inhibitors might provide new therapeutic approaches to treat cancers and overcome limitations of existing tubulin interactive drugs.[3]

Our previously described 2- and 7-phenylpyrrolo-quinolinones (2- and 7-PPyQs) (Figure 1) are a class of antiproliferative agents acting as tubulin polymerization inhibitors by binding at the colchicine site of β-tubulin.[4,5] Members of the less cytotoxic 2-PPyQ family were also found to exhibit interesting in vitro and in vivo antiangiogenic properties.[6]

The first generation of 7-PPyQs showed interesting in vitro biological properties. Some derivatives had micromolar GI_{50} values and good antitumor activity in vivo.[5] The second generation, characterized by alkyl substitutions at the pyrrolic nitrogen, showed increased cytotoxicity with nanomolar GI_{50} values, and these compounds overcame cross resistance observed with the clinically used agents vincristine and paclitaxel.[7] In the latter series, the 3*N*-cyclopropylmethyl 7-PPyQ derivative (**22**, MG 2477) was taken as lead compound due to its very strong cytotoxicity (nanomolar range GI_{50} values) and its potent interaction with tubulin. Its activities as an inhibitor of tubulin polymerization and of colchicine binding to tubulin were similar to those of the reference compound combretastatin A-4 (CA-4, Figure 1) (0.90 μM assembly IC_{50} and 83% inhibition of colchicine binding for 22 versus values of 1.1 μM and 99%, respectively, for CA-4).[7]

In an effort to produce additional highly active compounds, numerous related analogues were synthesized, and the effects of a variety of substitutions at diverse positions of the 3*H*-

pyrrolo[3,2-*f*] quinolin-9-one nucleus (PyQ) were evaluated.[8] In the present study, a number of new 7-PPyQ derivatives were designed, synthesized, and evaluated in cellular cytotoxicity and tubulin inhibition assays, resulting in the discovery of potent amidic derivatives. Furthermore, our recent study indicated that **22** is highly effective in reducing cell viability, and the reduced survival of A549 cells is associated with an initial autophagy that may be mediated by inhibition of the PI3K/Akt/mTOR pathway.[9] This pathway plays a variety of physiological roles, including regulation of cell growth and proliferation, and is perhaps the most frequently disregulated pathway in human cancers conferring aggressiveness and poor prognosis.[10,11] These findings prompted us to determine whether the new 7-PPyQ derivatives also interfere with the PI3K/Akt pathway and exert kinase inhibitory activity.

RESULTS AND DISCUSSION

Chemistry

The general method leading to the novel 3-substituted 7-PPyQ compounds was previously reported[7] and consists of four steps as described in Scheme 1A. First, commercially available 5-nitroindole (**1**) was subjected to an N-alkylation or acylation reaction using appropriate halogenated compounds to obtain the nitroindole derivatives **2a–f**. The same reaction conditions were used with all chloro and bromo compounds and with ethyl acrylate in anhydrous DMF in the presence of NaH at room temperature, resulting in high yields of the reaction products. The catalytic reduction (Pd/C 10%, H_2 at atmospheric pressure, ethyl acetate) of intermediates **2a–d** gave aminoindoles **3a–d** in almost quantitative yields. In the case of **2f** (and for **2e** not shown) the catalytic procedure furnished the partially reduced derivative **6f** as described in Scheme 1B. To obtain fully aromatic aminoindoles **3e** and **3f**, a chemical reduction with $SnCl_2$ in methanol at reflux was necessary but resulted in lower final yields. The condensation reactions of aminoindoles **3a** and **3c–f** with ethyl benzoylacetate and of **3b** with ethyl dimethoxybenzoylacetate were carried out in absolute ethanol at reflux and yielded the acrylate derivatives **4a–f** as crude material, which first had to be purified by silica gel column chromatography and then submitted to thermal cyclization in boiling diphenyl ether (250 °C) to obtain **5a–f**. Cyclization products **5a–f** were further purified by recrystallization or column chromatography, with their purity verified by HPLC (>95%). In Scheme 1B, **6f** obtained by means of catalytic reduction of the nitro compound **2f** was reacted with ethyl benzoylacetate (**7f**) and thermally cyclized to the partially hydrogenated 7-PPyQ **8f**.

As shown in Scheme 2, the chemical transformations of the two previously reported 3-ethyl 7-PPyQs (**19**),[6] ethyl 3*N*-propanoate (**21**)[7] and of some 7-PPyQs described in Scheme 1 are shown. In Scheme 2A, **19**, when reacted with CH_3I, C_4H_9Br or $NO_2C_6H_5CH_2Br$ in anhydrous DMF and in the presence of NaH, yielded the respective mixed ethers **9–11** as the only reaction products, bearing the alkoxylic function in the 9 position. Similarly, **19** reacted with benzylchloroformate and NaH in methanol at 0 °C to furnish the 9-substituted carbonate ester **12** as the only reaction product. In Scheme 2B, in order to obtain compound **13**, the 6*N*-methyl derivative of **19**, important for our SAR analysis, the 9-methoxy-PPyQ **9** was refluxed with excess CH3I for 2 h. This reaction provided the intermediate quinolinium

iodide, which was not isolated but yielded **13** by treatment of the reaction mixture with 1 N NaOH at reflux.[12] The exact structures with the precise alkylation or acylation sites in **9–13** were obtained by 1D and 2D NMR HMBC experiments (Figures 2–4 in Supporting Information).

As shown in Scheme 2C, the ethyl 3*N*-propanoate **21**[8] was reduced with $LiAlH_4$ in anhydrous THF to yield the corresponding alcohol **14**. Alternatively, **21** underwent alkaline hydrolysis in 1 N NaOH in methanol to provide the corresponding carboxylic acid **15**. Similarly, **5d** yielded acid **16** (Scheme 2D).

As shown in Scheme 2E, the 3*N*-propanenitrile **5c**, prepared as described in Scheme 1, was reduced with $NaBH_4$ in the presence $CoCl_2$ catalyst in methanol and in the presence of an equimolar quantity of di-*tert*-butyl dicarbonate. This somewhat laborious procedure[13] was superior to others[14,15] because the ^{t}Boc protected 7-PPyQ amine **17** was obtained as a solid product, which was more easily isolated from the reaction mixture than the free amine. Compound **17** was dissolved in an ethyl acetate/methanol mixture, and excess HCl dry gas was bubbled through the mixture to yield the hydrochloride compound **18** as a beige powder. 1D and 2D NMR spectrometry and absorption spectroscopy indicated that compound **18** was in the form of 9-hydroxypyrroloquinoline (Figures 7–10 in Supporting Information). We speculate that the hydroxylic form was obtained because of the treatment with HCl gas (see Experimental Section). This was confirmed through an investigation of the behavior of compound **18** in aqueous solution as a function of pH. On the basis of ^{1}H NMR and UV–vis spectra, it was observed that the two quinolinonic and hydroxyquinolinic tautomers interconvert in a pH dependent way: above pH 4 the keto tautomer predominates, while below pH 2 the enolic one is dominant (Figure 28 in Supporting Information). In the pH range 4–9, the spectra did not change, indicating that the compound was in the keto tautomer. Thus, at physiologic pH all 7-PPyQs, including compound **18**, are in the keto tautomer, with a carbonyl group at position 9 as previously proposed from the SAR findings.[8]

Biological Characterization

Antiproliferative Activity in Cellular Assays and SAR Analysis—On the basis of previous biological activity data on 7-PPyQs[7,10] and docking simulations of **22** in the colchicine site of tubulin,[9] the new compounds were designed to obtain additional SAR information by modifying the nature and size of substituents at the 3, 6, 7, and 9 positions of the PyQ tricycle. Evaluation of antiproliferative activities of **5a–f**, **8–16**, and **18** was performed with the 3-(4,5-dimethylthiazol-2-yl)-2,5-diphenyltetrazolium bromide (MTT) assay[16] against a panel of five solid tumor (HeLa, A549, HT-29, MCF-7, OVCAR-3) and nine leukemia cell lines (MOLT-3, CCRF-CEM, HL-60, K562, RS4;11, Jurkat, SEM, MV4;11, THP-1). GI_{50} values, the concentrations that inhibit cell growth by 50%, are presented in Table 1. Most of the novel 7-PPyQs possessed antiproliferative activity, inhibiting cell growth with nanomolar to micromolar GI_{50} values), except for the ethers **10** and **11** and the acids **15** and **16**. Of particular note were the subnanomolar GI_{50} values obtained with **5f**, but also with **5e** and **12**, in selected leukemic cell lines.

Overall, the most active of the new compounds was **5f** (average GI_{50}, 15 nM). It frequently had lower GI_{50} values than the previously described compounds **19–22**. Three additional compounds also had average GI_{50} values of <150 nM: **5e** (22 nM), **12** (22 nM), and **14** (120 nM). GI_{50} values below 100 nM in at least three cells lines were also observed with compounds **5c**, **8f**, and **9**. In an attempt to razionalize structure–antiproliferative activity relationships, the 7-PPyQs mentioned here and the corresponding previously described active 3-alkyl derivatives were ordered into four subsets on the bases of length, chemical nature, and size of the various substitutions, as depicted in Scheme 3. The first three subsets were selected by taking in consideration the substitutions at position 3, in comparison with previously described potent 3*N*-alkyl substituted 7-PPyQs, compounds **19** (3-ethyl), **20** (3-propyl), and **22** (3-cyclopropylmethyl).[7] The fourth subset includes compounds obtained by modifying the 9 position of compound **19** (9-C=O) to confirm the requirement for the carbonyl as a hydrogen bond acceptor in the active site on tubulin. Furthermore, the 6 position of **19** was methylated to gain SAR information on the 6 position and the phenyl at the 7 position was replaced by a dimethoxyphenyl moiety to determine the importance of the size and nature of the aryl substituent at that position.

From a comparison of the first two subsets and their GI_{50} values (Table 1), cytotoxicity changes with the lipophilic character of the chain at the 3 position: the shorter and more polar is the chain, the weaker is the cytotoxicity, with the acids **15** and **16** being completely inactive.

In the third subset, an important chemical modification was introduced, consisting of an amidic connection between the indole ring and the side chain, to yield the amidic derivatives **5e** and **5f**. This chemical modification provided compounds with potent antiproliferative activities, comparable with the activity obtained with parent **22**. As noted above, these two compounds, along with compound **12**, had the strongest antiproliferative activity. The fourth subset includes analogues of compound **19** designed and synthesized in order to evaluate substitutions at the 9 position. Previously, we had stressed the essential role of the carbonyl moiety for the antitubulin activity of 7-PPyQs in comparison with the corresponding phenylpyrroloquinoline lacking this moiety,[7] but we had not evaluated the effect of other substituents at position 9. The substituents in **9**, **10**, and **11**, lacking a carbonyl moiety, had reduced or minimal antiproliferative activity as compared with **19**. Moreover, as expected, the GI_{50} progressively decreased with steric hindrance in comparing the methyl derivative **9** with **10** and **11** with still bulkier groups. However, the bulkiest 9-benzyl carbonate derivative **12** was found to be a highly cytotoxic agent because it probably decomposed to **19** in the intracellular environment. Indeed, it is stable as a solid, while in dilute aqueous solution it quickly decomposes to the corresponding phenylpyrroloquinolinone (as proved by HPLC). Moreover, this degradation is in agreement with the data obtained with tubulin (Table 3) that show compound **12** to be as strong an inhibitor as its parent compound **19**.

To obtain data regarding the 6 position of the 7-PPyQs, we synthesized and evaluated compound **13** by attaching a methylic group at the quinolinic nitrogen of **19**. This led to a compound with reduced antiproliferative activity with respect to the unsubstituted parent compound **19**. Finally, in order to get further information about the size and nature of the

pocket in tubulin with which the phenyl at position 7 interacts, **5b** was designed and synthesized. In this compound the unsubstituted 7-phenyl group of **19** was replaced by a dimethoxyphenyl group. This compound was relatively inactive, leading us to conclude that the bulkier substituent led to a compound with a weaker interaction with tubulin. This is in agreement with what was previously observed with the series of 3-unsubstituted 7-PPyQs.[5]

We therefore conclude that the 7-PPyQ molecule tolerates very few chemical modifications and that for significant cytotoxicity only the 3-N position allows for a limited variety of substitutions. Substituents at this position require appropriate characteristics of size and polarity, and 3*N*-acylation yielded the highly active amidic compounds **5e** and **5f**. Due to its broad spectrum of potent antiproliferative activity, **5f** was selected for further biological investigations on mechanism of action and for comparison with **22**.

Evaluation of Antiproliferative Activity of 5f in Nontumor Cells—We investigated the effect of **5f** and of **22** in human lymphocytes and human umbilical vein endothelial cells (HUVECs), isolated from healthy donors. As shown in Table 2, in both unstimulated and mitogen-activated lymphocytes, the two compounds showed low toxicity as compared with their potent activity in cancer cells. Somewhat greater cytotoxicity was observed in HUVECs when incubated with both compounds. In both cases the GI_{50} values of 7.8 (**22**) and 22.1 (**5f**) μM are significantly higher than the values obtained in the panel of tumor cells. These results suggest that both compounds may have a preferential selectivity toward cancer cells, especially **5f**.

5f Binds to the Colchicine Site of Tubulin and Inhibits Tubulin Assembly—In previous studies we found that the antiproliferative activity of other 7-PPyQs resulted from an interaction with tubulin at the colchicine site.[17–20] Thus, the compounds of this new series were evaluated for their inhibition of tubulin polymerization and for their ability to inhibit [^{3}H]colchicine binding to tubulin. For comparison, CA-4, a drug candidate in clinical trials in its phosphorylated form, was evaluated as a reference compound in simultaneous experiments (Table 3). CA-4 is a well described, highly potent competitive inhibitor of the binding of colchicine to tubulin.[17] In the assembly assay,[18] compound **5f** was found to be the most active of the new agents as an inhibitor of tubulin polymerization, with an IC_{50} (0.99 μM) comparable with that of both **22** (0.90 μM) and CA-4 (1.20 μM). In the [^{3}H]colchichine binding assay,[19] compound **5f** was the most active new derivative (69% inhibition at 5 μM), although this activity was somewhat less than that observed with both 22 and CA-4 (83% and 99% inhibition, respectively, at 5 μM). There was good correlation between inhibition of tubulin polymerization, inhibition of colchicine binding, and antiproliferative activity of the new derivatives, in particular since **5f** had the highest activity in all three assays. Note that compound **12** behaved similarly to **19**, which is in a good correlation with antiproliferative activity data. Of the compounds examined with tubulin, somewhat decreased activity was observed with **13** and **14** with respect to **5f**. These compounds inhibited assembly with IC_{50} values of 1.8 and 1.2 μM, respectively. These compounds were also less active as inhibitors of colchichine binding than **5f** and CA-4, 61% and 40% inhibition, respectively.

As previously described for **22**, to further examine the competitive binding of **5f** with colchicine in the active site of the 1SA0 structure, computer-based docking of **5f** was performed using the MOE-Dock program.[21,22] Figure 2 depicts the binding mode of **5f** in the presumptive colchicine site. In particular, the colchicine site is mostly buried in the intermediate domain of the β-subunit, even if colchicine can also interact with loop T5 of the neighboring α-subunit (Figure 2), consistent with the observation that colchicine stabilizes the tubulin heterodimer. Not surprisingly, the accommodation of **5f** in the colchicine cleft is similar to that previously described for **22**.[9] Also in this case, docking simulations showed that, similar to colchicine and **22**, **5f** also can be accommodated in the same hydrophobic cleft, adopting an energetically stable conformation. Moreover, the most stable conformation of **5f** reproduced the scheme of chemical interactions (predominantly through hydrophobic interactions with Val181, Ala250, Cys241, Ala316, Val318, and Ile378 of the β-subunit) observed for colchicine, together with a similar interaction with the bordering T5 loop of α-tubulin, demonstrating a plausible competitive mechanism of action at the colchicine site.

5f Induces Cell Cycle Arrest at the G2/M Phase of the Cell Cycle—The effect of **5f** on cell cycle progression was examined by flow cytometry in the HeLa, Jurkat, and RS4;11 cell lines after a 24 h treatment with difierent concentrations of the agent (Figure 3). For all cell lines, the treatment resulted in the accumulation of cells in the G2/M phase of the cell cycle. In particular, the increase of G2/M cells began at 30 nM and was concentration dependent until a plateau was reached at 60 nM. In the three cell lines, G2/M arrest was accompanied by a concomitant reduction in the proportion of cells in the G1 phase. Only in HeLa cells was a significant decrease of S phase cells observed.

We next studied the association between **5f**-induced G2/M arrest and alterations in the expression of proteins that regulate cell division. The cdc2/cyclin B complex controls both entry into and exit from mitosis. Phosphorylation of cdc2 on Tyr15 and phosphorylation of cdc25C phosphatase on Ser216 negatively regulate the activation of the cdc2/cyclin B complex. Thus, dephosphorylation of these proteins is needed to activate the cdc2/cyclin B complex. Cdc25C is a major phosphatase that dephosphorylates the site on cdc2 and autodephosphorylates itself. Phosphorylation of cdc25C directly stimulates both its phosphatase and autophosphatase activities, a condition necessary to activate cdc2/cyclin B on entry of cells into mitosis.[23–25] As shown in Figure 4, in Jurkat cells treatment with **5f** at either 0.1 or 1 μM caused no significant variations in cyclin B expression after a 24 h treatment. However, we observed a marked decrease in the expression of the phosphorylated form of cdc2 (Tyr15) and that of cdc25C, in particular with 1 μM **5f**. These data, along with accumulation of cells in the G2/M phase, suggest that **5f**-induced G2/M arrest was not due to defects in G2/M regulatory proteins but rather is closely linked with acceleration of entry into mitosis.

In addition to the analysis of proteins that control cell cycle checkpoints, we also examined the phosphorylation of the tumor suppressor p53 at Ser15 after treating Jurkat cells with **5f**. It is well-known that prolonged mitotic arrest induces DNA damage and, consequently, the phosphorylation of p53 at Ser15 that leads to p53 stabilization and accumulation.[26,27] As shown in Figure 4, we detected a concentration-dependent marked increase of p53-Ser15

that is particularly evident with 1 μM **5f**. At the same time, we also observed a marked increase in the phosphorylation of histone γH2A.X at Ser139, which is an early sensitive indicator of DNA damage.[28]

5f Induces Apoptotic Cell Death—To characterize the mode of cell death induced by **5f**, biparametric flow cytometric analysis with annexin-V/propidium iodide (PI) was performed on difierent cell lines. PI binds to DNA and is permeable only in dead, nonapoptotic cells, while annexin-V has high affinity for phosphatidylserine (PS) that is exposed only on the outer membrane leaffet of apoptotic cells. Thus, the dual staining permits quantitation of live cells (annexin-V^-/PI^-), early apoptotic cells (annexin-V^+/PI^-), late apoptotic cells (annexin-V^+/PI^+), and necrotic cells (annexin-V^-/PI^+). As shown in Figure 5, **5f** induced an increase in the annexin V^+ fraction, and thus of apoptosis, in a concentration dependent manner in HeLa cells (Figure 5A) and in leukemic cell lines such as Jurkat (Figure 5B), RS4;11 (Figure 5C), and K562 (Figure 5D).

To evaluate which caspases were involved in the apoptotic cell death induced by **5f**, we analyzed Jurkat cell protein extracts by immunoblot. After a 24 h treatment with **5f**, we observed the cleavage of activator caspases 2, 8, and 9 (Figure 6A). Moreover, we observed also the activation of the effector caspase-3 and the subsequent cleavage of its substrate PARP.

The intracellular apoptotic program can be modulated by the expression of Bcl-2 family proteins that include both proapoptotic and antiapoptotic members. Bcl-2 family proteins are the main regulators of the mitochondrial apoptotic pathway through the control of mitochondrial membrane permeability and release of cytochrome *c*.[29] It is well-known that cancer cells express high levels of Bcl antiapoptotic proteins such as Bcl-2, Bcl-XL, Mcl-1, Bcl-w, Boo/Diva, Bcl-B, and NR-13 and that microtubule targeting agents induce the downregulation of the Bcl-2 antiapoptotic protein, thus promoting apoptosis.[30,31] As shown in Figure 6B in Jurkat cells, after a 24 h incubation, compound **5f** induced a significant decrease in Bcl-2, Bcl-XL, and Mcl-1 expression at the lower concentration (0.1 μM) examined. These results are in agreement with recent studies that point out the importance of Mcl-1 in cell death induced by antitubulin agents.[32] In addition, Mcl-1 appears to play a major role in cancer cell survival, especially in leukemia cells. Thus, this observation with **5f** suggestes that the agent could be an attractive pharmacological tool for induction of Mcl-1 depletion.[33,34]

Survivin is a member of IAP family (inhibitor of apoptosis protein).[35] In general, the IAPs function through direct interactions to inhibit the activity of several caspases, including caspase-3, caspase-7, and caspase-9, and IAPs thereby inhibit the processing and activation of these enzymes.[36] We found that survivin was phosphorylated on Thr32 following treatment with **5f**. This effect is consistent with cell cycle arrest in mitosis and is shared by various antimitotic drugs.[37,38]

5f Induces Inhibition of the PI3K/Akt/mTOR Pathway—Recently, we identified **22**, a structural analogue of **5f**, as a potent antimitotic compound that might interfere with the PI3K/Akt/mTOR pathway.[9] Therefore, we evaluated the effect of compound **5f** on this

pathway in Jurkat cells, which are a PTEN-null, T-cell acute lymphoblastic leukemia cell line. As shown in Figure 7, **5f** induced the reduction of the p85 regulatory subunit of PI3K and caused the decrease of the phosphorylated (active) forms of mTOR (Ser2448) and AKT (Ser473, Thr308). **5f** treatment also induced a decrease in the phosphorylation of mTOR downstream targets such as S6 kinase (Ser240/244), 4E-BP1 (Ser65), and GSK3 (Ser21).

5f Inhibits Enzymatic Activity of Difierent Protein Kinases—Because of the significant effect of **5f** on the PI3K/Akt/mTOR pathway, we performed DiscoveRx KINOMEscan[39] profiles on a panel of 386 distinct human protein kinases at 1 μM **5f** (Figure 8). The percent inhibition at this concentration is represented with red dots (Figure 8A) that, depending on their size, indicate the residual activity of the kinase.

With this screening platform, we found that **5f** at 1 μM induced over 50% inhibition of 23 protein kinases (Figure 8B). We found that **5f** did not directly inhibit PI3K, Akt, and mTOR. However, among the inhibited kinases were AURKA, FLT3, GSK3A, MAP3K, MEK4, RSK2, RSK4, PLK4, ULK1, and JAK2 that in cells could interact with the PI3K/Akt/mTOR pathway. These results suggest that suppression of these kinases could contribute to the high cytotoxicity caused by **5f**.

To better understand the apparently unpredictable behavior of **22** and **5f** as protein kinase inhibitors, a computer-based automated docking of both compounds was performed as described in detail in the Experimental Section. For this computational study, we selected from among the kinases that were inhibited more than 50% (Figure 8B) and whose crystallographic structures were deposited in the Protein Data Bank. As reported in detail in the Experimental Section, the ATP binding sites of five protein kinases (RSK2, PLK4, FLT3, JAK1, and GSK3)[40–42] were used to explore the binding of both **22** and **5f**. We found that these 7-phenylpyrrolo-quinolinones could be readily accommodated in the ATP binding clefts of all selected protein kinases but that the ligand–kinase stabilization energy associated with the binding of **5f** was much higher (around 4–9 kcal/mol higher) as compared with **22**. In particular, the experimental inhibitory activity shown by **5f** can be attributed to the presence of the amide moiety at the 3-position through the formation of a strong H-bonding interaction with the side chain of amino acids located inside the ATP binding cavity (Figure 9). In Table 4 are summarized the most relevant binding features of **5f** with the five selected protein kinases.

5f Synergizes with Conventional Chemotherapeutic Agents in Inhibiting Leukemia Cell Proliferation—Since **5f** induced a strong decrease in cancer cell proliferation, we evaluated whether **5f** had promise when used in combination with commonly used chemotherapeutics in leukemia treatment. To this end, three difierent leukemia cell lines, two glucocorticoid-resistant (Jurkat, THP-1) and one glucocorticoid-sensitive (MV4;11) were treated for 48 h with **5f** in combination with selected chemotherapeutic agents (i.e., dexamethasone, daunorubicin, and Ara-C) used frequently to treat leukemic patients. Compound **5f** was combined with difierent drugs at a fixed molar combination ratio, and cell viability was analyzed by the MTT assay (Figure 10 and Supporting Information Figure 29).

As described above, **5f** alone had significant cytotoxicity when used as a single agent (Table 1). When used in combination with chemotherapeutic drugs, we observed a synergistic increase in cytotoxicity, as demonstrated by combination index (CI) values obtained by the analytic method of Chou and Talalay.[43–45] As summarized in Table 5, in which CI values calculated at the GI_{50}, GI_{75}, and GI_{90} values are shown, in almost all cases, but not with Jurkat cells for Ara-C treatment, **5f** and the selected chemotherapeutic drugs acted in a synergistic fashion (CI < 1). Moreover, in the glucocorticoid resistant cells, Jurkat and THP-1, **5f** was able to restore glucocorticoid sensitivity, suggesting that **5f** might be able to optimize the efficacy of existing therapies for leukemia.

CONCLUSION

A series of new 7-PPyQs was efficiently synthesized and biologically evaluated as anticancer agents. With respect to the previously reported analogues, the new compounds were further modified at the 3, 6, 7, and 9 positions. Our findings reported here show that the only chemical modifications tolerated by the 7-PPyQ pharmacophore without a major loss in antiproliferative potency occur at the 3N position. However, substituents at this position must show suitable size and polarity properties in order to preserve the strong cytotoxicity of the most active compounds. This was observed, for example, with compounds **20**, **5a**, and **14** (Table 1), in which the potency decreased in the following order: **20** (3*N*-propyl, low nanomolar GI_{50}) > **14** (3*N*-propyl alcohol, high nanomolar GI_{50}) > **5a** (3*N*-ethyl alcohol, high micromolar GI_{50}). Compound **15** (N-propanoic acid) and compound **16** (N-ethanoic acid) were both inactive. Among all compounds reported here, the amidic derivatives **5e** and **5f**, obtained by acylation of the pyrrolic N, showed very high cytotoxicity.

Importantly, when tested in human noncancer cell lines, **22** and especially **5f** showed very low toxicity compared with tumor cell lines (Table 2).

All 7-PPyQs examined share the same primary mechanism of action, inhibition of tubulin polymerization by binding in the colchicine site (Table 3). In general, their potency as antitubulin agents correlated well with their potency as antiproliferative agents. The effect of **5f** on cell cycle progression was examined with three cell lines (Figure 2), and the agent caused G2/M arrest. We showed alterations in expression of proteins that regulate cell division (Figure 3). These studies indicated that **5f** at 1 μM induced G2/M arrest not because of defects in G2/M regulatory proteins but rather because there was an acceleration of entry into mitosis (Figure 4). As observed in some cancer cell lines, in a concentration dependent manner, **5f**, like **22**, caused cell death by apoptosis involving activator caspases 2, 8, and 9, activation of the effector caspase-3, and subsequent cleavage of PARP. Moreover, as with other microtubule targeting agents, at 0.1 μM in Jurkat cells, **5f** induced downregulation of the antiapoptotic proteins Bcl-2, Bcl-XL, and particularly Mcl-1, which is a key factor governing cell survival and often overexpressed in cancer cells. Also, as noted with various antimitotic drugs, survivin was found to be phosphorylated upon treatment with **5f**, additional evidence of cell cycle arrest in mitosis (Figure 5).

Another interesting finding of our work is that **5f** modulates the PI3K/Akt/mTOR pathway which plays a major role in tumorigenesis and progression, since it is often hyperactivated in many types of tumors. Although this observation was already described by our group in A549 cell lines with compound **22**, in this work we show this effect was maintained also in PTEN null cell line Jurkat. In this context it is worthwhile to note that PTEN mutations are associated with bad prognosis and that PTEN null tumors are particularly aggressive due to the strong activation of PI3K/Akt/mTOR pathway. Thus, the therapeutic potential of **5f** with respect to other antimitotic compounds could be strongly enhanced and extended to difierent kinds of tumor.

By a KINOMEscan analysis with 1 μM **5f**, we found greater than 50% inhibition of 23 kinases (Figure 8B), but there was no direct inhibitory effect on the enzymatic activity on PI3K, Akt, and mTOR. Therefore, our results indicated that a simple chemical modification made by linking an acyl side chain to the pyrrolic nitrogen endowed this compound class with a kinase inhibiting activity and that suppression of the activity of selected kinases might contribute to the high cytotoxicity of **5f**.

Finally, **5f** sensitized leukemia cell lines to the action of frequently used chemotherapeutic drugs, leading to cell death in a synergistic way. This effect was observed with agents with difierent mechanisms of action. In particular, we observed that **5f** was able to restore the activity of dexamethasone in glucocorticoid resistant cells (Jurkat and THP-1). If confirmed in planned in vivo studies, this would be a valuable property of **5f**.

EXPERIMENTAL SECTION

Materials and Methods

Melting points were determined on a Buchi M-560 capillary melting point apparatus and are uncorrected. Infrared spectra were recorded on a PerkinElmer 1760 FTIR spectrometer with potassium bromide pressed disks; all values are expressed in cm^{-1}. UV–vis spectra were recorded on a Thermo Helyos α spectrometer. ^{1}H NMR spectra were determined on Bruker 300 and 400 MHz spectrometers, with the solvents indicated; chemical shifts are reported in δ (ppm) downfield from tetramethylsilane as internal reference. Coupling constants are given in hertz. In the case of multiplets, chemical shifts were measured starting from the approximate center. Integrals were satisfactorily in line with those expected on the basis of compound structure. Elemental analyses were performed in the Microanalytical Laboratory, Department of Pharmaceutical Sciences, University of Padova, on a PerkinElmer C, H, N elemental analyzer model 240B, and analyses indicated by the symbols of the elements were within ±0.4% of the theoretical values. Analytical data are presented in detail for each final compound in the Supporting Information. Mass spectra were obtained on a Mat 112 Varian Mat Bremen (70 eV) mass spectrometer and Applied Biosystems Mariner System 5220 LC/MS (nozzle potential 140 eV). Column flash chromatography was performed on Merck silica gel (250–400 mesh ASTM); chemical reactions were monitored by analytical thin-layer chromatography (TLC) on Merck silica gel 60 F-254 glass plates. Solutions were concentrated on a rotary evaporator under reduced pressure. Starting materials were purchased from Sigma-Aldrich and Alfa Aesar, and solvents were from Carlo Erba, Fluka

and Lab-Scan. DMSO was obtained anhydrous by distillation under vacuum and stored on molecular sieves.

The purity of new tested compounds was checked by HPLC using the instrument HPLC VARIAN ProStar model 210, with detector DAD VARIAN ProStar 335. The analysis was performed with a flow of 1 mL/min, a C-18 column of dimensions 250 mm × 4.6 mm, a particle size of 5 μm, and a loop of 10 μL. The detector was set at 300 nm. The mobile phase consisted of phase A (Milli-Q H_2O, 18.0 MΩ, TFA 0.05%) and phase B (95% MeCN, 5% phase A). The gradient elution was performed as reported: 0 min, % B = 10; 0–20 min, % B = 90; 20–25 min, % B = 90; 25–26 min, % B = 10; 26–31 min, % B = 10.

General Procedure for the Synthesis of 1*N*-Substituted Nitroindoles (2a–f)

As a typical procedure, the synthesis of 2-(5-nitro-1*H*-indol-1-yl)ethanol **2a** is described in detail. Into a two-necked 50 mL round-bottomed flask, 0.888 g (37 mmol) of NaH, 60% dispersion in mineral oil, was placed and washed with toluene (3 × 10 mL). With stirring, a solution of commercial 5-nitroindole **1**, 1.50 g (9.25 mmol) in 5 mL of anhydrous DMF, was dropped into the flask, and the initial yellow color changed to red with the formation of H_2 gas. After 30 min at room temperature, a solution of 2-bromoethanol, 0.981 mL (13.87 mmol; d = 1.763 g/mL) in 1 mL dry DMF, was added, and the reaction mixture was left to stir for 24 h. The reaction was monitored by TLC analysis (eluent toluene/*n*-hexane/ethyl acetate, 1:1:0.3). At the end of the reaction, 25 mL of water was added, and the solvent was evaporated under reduced pressure, leaving a residue, which was extracted with ethyl acetate (3 × 50 mL). The organic phase, washed with water and dried over anhydrous Na_2SO_4, was concentrated under vacuum giving a crude yellow solid (1.898 g). This crude product was purified with a silica gel chromatographic column (d 3 cm, l 35 cm, 230–400 mesh, eluent ethyl acetate/*n*-hexane, 7:3), yielding 1.587 g of a pure yellow solid.

2-(5-Nitro-1*H*-indol-1-yl)ethanol (2a)

Yield 82.2%; R_f = 0.31 (ethyl acetate/*n*-hexane 7:3); mp = 82 °C; ^{1}H NMR (400 MHz, DMSO-d_6) δ = 3.86 (q, 2H, J = 5.23 Hz, CH_2-CH_2-OH), 4.44 (t, 2H, J = 5.23 Hz, CH_2-CH_2-OH), 5.07 (t, 1H, J = 5.23 Hz, OH), 6.87 (dd, 1H, J = 3.18 and J = 0.59 Hz, 3-H), 7.76 (d, 1H, J = 3.18 Hz, 2-H), 7.82 (d, 1H, J = 9.15 Hz, 7-H), 8.15 (dd, 1H, J = 9.15 and J = 2.30 Hz, 6-H), 8.70 (d, 1H, J = 2.30 Hz, 4-H); ^{13}C NMR (101 MHz, DMSO-d_6) δ = 49.08 (NCH_2CH_2OH), 61.07 (NCH_2CH_2OH), 103.24 (3-C), 112.36 (7-C), 116.93 (6-C), 119.24 (4-C), 134.12 (2-C), 135.22 (3a-C), 138.24 (7a-C), 143.16 ppm (5-C). HRMS (ESI-MS, 140 eV): m/z [M + H$^+$] calculated for $C_{10}H_{11}N_2O_3^+$, 207.2054; found, 207.1987.

1-(Cyclopropylmethyl)-4-nitro-1*H*-indole (2b)

Compound **2b** was prepared as for compound **2a**, and the analytical data are reported in ref 7.

3-(5-Nitro-1*H*-indol-1-yl)propanenitrile (2c)

Compound **2c** was prepared as for compound **2a** by reacting 0.720 g of NaH 60% (30 mmol) and 1.621 g (10.0 mmol) of 5-nitroindole 1 dissolved in 5 mL of DMF and 1.24 mL of 3-bromopropionitrile (15 mmol, d = 1.615 g/mL). Reaction time 5 h (TLC ethyl acetate/*n*-

hexane/toluene, 1:1:1). A solid product (2.564 g) was obtained. Yield 99%; R_f = 0.27 (toluene/*n*-hexane/ethyl acetate, 1:1:1); ^{1}H NMR (400 MHz, DMSO-d_6) δ = 3.10 (t, 2H, *J* = 6.60 Hz, NCH_2CH_2CN), 4.61 (t, 2H, *J* = 6.52 Hz, NCH_2CH_2CN), 6.81 (dd, 1H, *J* = 3.24 Hz and *J* = 0.8 Hz, 3-H), 7.72 (d, 1H, *J* = 3.31 Hz, 2-H), 7.83 (dt, 1H, *J* = 9.13 Hz and *J* = 0.7 Hz, 7-H), 8.06 (ddd, 1H, *J* = 9.08 Hz, *J* = 2.29 Hz and *J* = 0.25 Hz, 6-H), 8.59 ppm (dd, 1H, *J* = 2.24 Hz and *J* = 0.25 Hz, 4-H); ^{13}C NMR (101 MHz, DMSO-d_6) δ = 19.08 (NCH_2CH_2CN), 42.07 (NCH_2CH_2CN), 104.76 (3-C), 111.06 (7-C), 117.03 (6-C), 118.04 (4-C), 119.10 (CN), 132.76 (2-C), 132.76 (3a-C), 139.07 (7a-C), 141,48 ppm (5-C). HRMS (ESI-MS, 140 eV): *m/z* [M + H^+] calculated for $C_{11}H_{10}N_3O^+$, 216.2155; found, 216.1290.

Ethyl 2-(5-Nitro-1*H*-indol-1-yl)acetate (2d)

Compound **2d** was prepared as for compound **2a** by reacting 0.445 g of NaH 60% (18.51 mmol) and 1.00 g (6.17 mmol) of 5-nitroindole **1** dissolved in 10 mL of toluene and 1.5456 g (9.25 mmol, *d* = 1.506 g/L) of bromoethyl acetate in 5 mL toluene. Reaction time was 4 h by TLC analysis (ethyl acetate/*n*-hexane/toluene, 1:1:1). After extraction, 1.400 g of the crude material was obtained, which was chromatographed on a silica gel column (*d* = 3 cm, *l* = 30 cm, 230–400 mesh, ethyl acetate/*n*-hexane/toluene, 1:1:1) giving 0.665 g of a pure bright white solid. Yield 47.5%; mp = 52–53 °C; R_f = 0.63 (eluent ethyl acetate/*n*-hexane/toluene, 1:1:1); ^{1}H NMR (300 MHz, DMSO-d_6) δ = 1.21 (t, 3H, *J* = 7.05 Hz, $-OCH_2CH_3$), 4.17 (q, 2H, *J* = 7.05 Hz, $-OCH_2CH_3$), 5.26 (s, 2H, NCH_2), 6.78 (dd, 1H, *J* = 3.24 Hz and *J* = 0.76 Hz, 3-H), 7.61 (d, 1H, *J* = 3.24 Hz, 2-H), 7.64 (d, 1H, *J* = 9.15 Hz and *J* = 0.76 Hz, 7-H), 8.04 (dd, 1H, *J* = 9.15 Hz and *J* = 2.28 Hz, 6-H), 8.58 ppm (d, 1H, *J* = 2.09 Hz, 4-H); ^{13}C NMR (75 MHz, DMSO-d_6) δ = 16.83 ($NCH_2COOCH_2CH_3$), 47.15 ($NCH_2COOCH_2CH_3$), 64.34 ($NCH_2COOCH_2CH_3$), 102.02 (3-C), 111.66 (7-C), 117.74 (6-C), 120.00 (4-C), 132.64 (2-C), 134.73 (3a-C), 137.98 (7a-C), 145.05 (5-C), 167.72 ppm ($NCH_2COOCH_2CH_3$). HRMS (ESI-MS, 140 eV): *m/z* [M + H^+] calculated for $C_{12}H_{13}N_2O_4^+$, 249.2421; found, 249.1497.

1-(5-Nitro-1*H*-indol-1-yl)propan-1-one (2e)

Compound **2e** was prepared as for compound **2a** by reacting 0.444 g of NaH 60% (18.50 mmol) and 1.00 g (6.17 mmol) of commercial 5-nitroindole (**1**) dissolved in 5 mL of anhydrous DMF and 0.808 mL (9.25 mmol, *d* = 1.059 g/mL) of propionyl chloride dissolved in 1 mL of anhydrous DMF. On addition of the propionyl chloride solution, a white precipitate formed. After about 1 h, the solution was cooled (ice bath) and treated with 15 mL of water to quench the excess NaH. The precipitate formed was collected by filtration under vacuum, washed several times with water, and desiccated under vacuum, yielding 0.920 g of a white crystalline compound. Yield 68%; R_f = 0.63 (ethyl acetate/*n*-hexane/toluene, 1:1:1); mp = 177 °C; ^{1}H NMR (400 MHz, DMSO-d_6) δ = 1.19 (t, 3H, *J* = 7.25 Hz, $C(O)CH_2CH_3$), 3.13 (q, 2H, *J* = 7.25 Hz, $C(O)CH_2CH_3$), 6.97 (d, 1H, *J* = 3.34 Hz, 3-H), 8.14 (d, 1H, *J* = 3.34 Hz, 2-H), 8.20 (dd, 1H, *J* = 9.29 Hz and *J* = 2.25 Hz, 6-H), 8.52 (dt, 1H, *J* = 9.29 Hz, 7-H), 8.58 ppm (d, 1H, *J* = 2.25 Hz, 4-H); ^{13}C NMR (101 MHz, DMSO-d_6) δ = 8.75 ($C(O)CH_2CH_3$), 28.97 ($C(O)\ CH_2CH_3$), 109.15 (3-C), 116.63 (7-C), 117.50 (4-C), 120.11 (6-C), 130.27 (2-C), 130.41 (3a-C), 138.41 (7a-C), 143.80 (5-C), 173.73 ppm

(NC(O)). HRMS (ESI-MS, 140 eV): *m/z* [M + H^+] calculated for $C_{11}H_{11}N_2O^+$, 219.1261; found, 219.1291.

Cyclopropyl(5-nitro-1*H*-indol-1-yl)methanone (2f)

Compound **2f** was prepared as for compound **2a** by reacting 0.445 g of NaH 60% (18.51 mmol) and 1.012 g (6.24 mmol) of 5-nitroindole **1** dissolved in 10 mL DMF and 1.10 mL of cylopropanecarbonyl chloride (12.20 mmol, *d* = 1.152 g/mL). Reaction time was 3 h, monitoring by TLC (ethyl acetate/*n*-hexane/toluene, 1:1:1). After extraction, 0.860 g of crude reaction product, a golden solid (70%), was obtained, which was chromatographed on a silica gel column (*d* = 3 cm, *l* = 35 cm, 230–400 mesh, ethyl acetate/*n*-hexane/toluene, 1:1:1) to yield 0.752 g of pure compound **2f**. Yield 52%; R_f = 0.62 (ethyl acetate/*n*-hexane/toluene, 1:1:1); mp = 45–48 °C; ^{1}H NMR (400 MHz, DMSO-d_6) δ = 1.17 (m, 4H, CH_2-CH_2), 2.77 (m, 1H, CH), 7.05 (dd, 1H, *J* = 3.81 Hz and *J* = 0.76 Hz, 3-H), 8.20 (dd, 1H, *J* = 9.15 Hz and *J* = 2.48 Hz, 6-H), 8.47 (d, 1H, *J* = 3.18 Hz, 2-H), 8.50 (d, 1H, *J* = 9.15 Hz, 7-H), 8.61 ppm (d, 1H, *J* = 2.48 Hz, 4-H); ^{13}C NMR (101 MHz, DMSO-d_6) δ = 15.14 (CH_2CH_2), 26.34 (CH), 101.99 (3-C), 113.14 (7-C), 115.82 (6-C), 118.34 (4-C), 133.84 (2-C), 134.72 (3a-C), 137.46 (7a-C), 144.04 (5-C), 172.01 ppm (NC(O)$CHCH_2CH_2$). HRMS (ESI-MS, 140 eV): *m/z* [M + H^+] calculated for $C_{12}H_{11}N_2O_3^+$, 231.2268; found, 231.1382.

General Procedure for the Synthesis of 1*N*-Substituted Aminoindoles 3a–d and 6f

As a typical procedure, the synthesis of 5-aminoindole **3a** is described in detail. Into a three-necked flask of 500 mL, previously dried in an oven, about 0.300 g of C/Pd 10% and approximately 60 mL of ethyl acetate were placed. After connecting the flask to an elastomer balloon containing hydrogen gas, the mixture was stirred at room temperature for 1 h in order to saturate the suspension of C/Pd with hydrogen. Then, 7.70 mmol (1.587 g) of nitroindole derivative **2a** in 15 mL of ethyl acetate was added dropwise to the suspension, and the mixture was stirred under hydrogen at atmospheric pressure and heated by means of an oil bath at 50–60 °C for 15 h, monitoring the progress of the reaction by TLC analysis (ethyl acetate/*n*-hexane, 7:3). At the end of the reaction, the mixture was filtered, and the solution was concentrated to dryness on a rotavapor to give 1.234 g of semisolid dark purple product.

2-(5-Amino-1*H*-indol-1-yl)ethanol (3a)

Yield 91%; mp = 124 °C; R_f = 0.20 (ethyl acetate/*n*-hexane, 7:3). ^{1}H NMR (400 MHz, DMSO-d_6) δ = 4.55 (q, 2H, *J* = 5.67 Hz, CH_2CH_2OH), 4.92 (bs, 2H, NH_2), 4.96 (t, 2H, *J* = 5.67 Hz, CH_2CH_2OH), 5.80 (t, 1H, *J* = 5.67 Hz, OH), 7.06 (dd, 1H, *J* = 3.25 Hz and *J* = 0.41 Hz, 3-H), 7.62 (dd, 1H, *J* = 8.79 Hz and *J* = 2.13 Hz, 6-H), 7.87 (d, 1H, *J* = 2.13 Hz, 4-H), 7.93 (d, 1H, *J* = 3.25 Hz, 2-H), 8.04 ppm (d, 1H, *J* = 8.79 Hz, 7-H); ^{13}C NMR (101 MHz, DMSO-d_6) δ = 47.34 (NCH_2CH_2OH), 60.77 (NCH_2CH_2OH), 100.34 (3-C), 105.72 (4-C), 111.34 (7-C), 113.75 (6-C), 127.96 (2-C), 128.14 (3a-C), 129.94 (7a-C), 142.90 ppm (5-C). HRMS (ESI-MS, 140 eV): *m/z* [M + H^+] calculated for $C_{10}H_{13}N_2O^+$, 177.2225, found:177.1565.

1-(Cyclopropylmethyl)-4-amino-1*H*-indole (3b)

Compound **3b** was prepared as for compound **3a**, and the analytical data are reported in ref 7.

3-(5-Amino-1*H*-indol-1-yl)propanenitrile (3c)

Compound **3c** was prepared as for compound **3a** by reacting 2.853 g (13.26 mmol) of nitroindole derivative **2c**, obtaining 1.842 g of a brown oil. Yield 97%; R_f = 0.11 (ethyl acetate/*n*-hexane/toluene, 1:1:1); ^{1}H NMR (400 MHz, DMSO-d_6) δ = 2.95 (t, 2H, *J* = 6.88 Hz, NCH_2CH_2CN), 4.36 (t, 2H, *J* = 6.88 Hz, NCH_2CH_2CN), 4.52 (s, 2H, NH_2), 6.17 (dd, 1H, *J* = 3.12 Hz and *J* = 0.85 Hz, 3-H), 6.55 (ddd, 1H, *J* = 8.73 Hz, *J* = 2.13 Hz and *J* = 0.33 Hz, 6-H), 6.70 (dd, 1H, *J* = 2.12 Hz and *J* = 0.61 Hz, 4-H), 7.21 (d, 1H, *J* = 3.12 Hz, 2-H), 7.23 ppm (dt, 1H, *J* = 8.74 Hz and *J* = 0.73 Hz, 7-H); ^{13}C NMR (101 MHz, DMSO-d_6) δ = 19.05 (NCH_2CH_2CN), 41.70 (NCH_2CH_2CN), 100.29 (3-C), 104.03 (4-C), 110.32 (7-C), 112.33 (6-C), 119.44 (CN), 128.45 (2-C), 129.70 (3a-C), 129.75 (7a-C), 142.19 ppm (5-C). HRMS (ESI-MS, 140 eV): *m/z* [M + H^+] calculated for $C_{11}H_{12}N_3^+$, 186.1031; found, 186.1012.

Ethyl 2-(5-Amino-1*H*-indol-1-yl)acetate (3d)

Compound **3d** was prepared as for compound **3c** by reacting 0.500 g of nitroindole derivative **2d** (2.01 mmol), obtaining 0.396 g of a violet solid. Yield 90%; R_f = 0.43 (*n*-hexane/ethyl acetate, 1:1); ^{1}H NMR (300 MHz, DMSO-d_6) δ = 1.21 (t, 3H, *J* = 7.05 Hz, CH_2CH_3), 4.13 (q, 2H, *J* = 7.05 Hz, CH_2CH_3), 4.50 (bs, 2H, NH_2), 4.95 (s, 2H, CH_2), 6.15 (dd, 1H, *J* = 3.05 Hz and *J* = 0.76 Hz, 3-H), 6.50 (dd, 1H, *J* = 8.58 Hz and *J* = 2.09 Hz, 6-H), 6.67 (d, 1H, *J* = 2.09 Hz and *J* = 0.52 Hz, 4-H), 7.02 (d, 1H, *J* = 8.77 Hz and *J* = 0.76 Hz, 7-H), 7.11 ppm (d, 1H, *J* = 3.05 Hz, 2-H); ^{13} C NMR (75 MHz, DMSO-d_6) δ = 15.22 ($NCH_2COOCH_2CH_3$), 45.53 ($NCH_2COOCH_2CH_3$), 64.22 ($NCH_2COOCH_2CH_3$), 101.20 (3-C), 104.73 (4-C), 112.74 (7-C), 114.01 (6-C), 126.06 (2-C), 127.94 (3a-C), 130.02 (7a-C), 143.06 (5-C), 168.25 ppm ($NCH_2COOCH_2CH_3$). HRMS (ESI-MS, 140 eV): *m/z* [M + H^+] calculated for $C_{12}H_{15}N_2O_2^+$, 219.2592; found, 219.2537.

(5-Aminoindolin-1-yl)(cyclopropyl)methanone (6f)

Compound **6f** was prepared as for compound **3a** by reacting 3.27 mmol (0.759 g) of 5-nitroindole **2f** at room temperature, obtaining 0.653 g of a slightly pink solid. Yield 98%; R_f = 0.37 (ethyl acetate/*n*-hexane, 8:2); mp = 159 °C; ^{1}H NMR (300 MHz, DMSO-d_6) δ = 0.80 (m, 4H, CH_2-CH_2), 1.85 (m, 1H, CH), 3.04 (t, 2H, *J* = 8.01 Hz, 2-H_2), 4.18 (t, 2H, *J* = 8.01 Hz, 3-H_2), 4.81 (bs, 2H, NH_2), 6.30 (dd, 1H, *J* = 8.58 Hz and *J* = 2.09 Hz, 6-H), 6.45 (s, 1H, 4-H), 6.71 ppm (d, 1H, *J* = 8.58 Hz, 7-H); ^{13}C NMR (75 MHz, DMSO-d_6) δ = 8.26 (CH_2CH_2), 14.02 (CH), 28.66 (3-C), 48.96 (2-C), 103.76 (4-C), 111.22 (7-C), 115.92 (6-C), 125.76 (3a-C), 127.42 (7a-C), 141.01 (5-C), 170.44 ppm ($NC(O)CHCH_2CH_2$). HRMS (ESI-MS, 140 eV): *m/z* [M + H^+] calculated for $C_{12}H_{15}N_2O^+$, 203.2598; found, 203.2524.

General Procedure for the Synthesis of 5-Aminoindoles 3e and 3f

As a typical procedure, the synthesis of 5-aminoindole **3e** is described in detail. Into a two-necked 50 mL round-bottomed flask, 0.350 g of 1-(5-nitro-1*H*-indol-1-yl)propan-1-one (**2e**)

(1.60 mmol), 1.809 g of $SnCl_2 \cdot 2H_2O$ (8.02 mmol), and 25 mL of methanol were added. The reaction mixture was refluxed for 3 h, and the reaction progress was monitored by TLC (*n*-hexane/ethyl acetate, 2:8). At the end, the solvent was evaporated, the residue was taken up with aqueous NaOH 20% (20 mL), and the resulting suspension was extracted with diethyl ether (4 × 50 mL). The combined extracts, washed with anhydrous Na_2SO_4, were evaporated to dryness on a rotary evaporator to yield 0.240 g of a semisolid yellow product.

1-(5-Amino-1*H*-indol-1-yl)propan-1-one (3e)

Yield 80%; mp = 132 °C; R_f = 0.27 (ethyl acetate/*n*-hexane/toluene, 1:1:1). ^{1}H NMR (400 MHz, DMSO-d_6) δ = 1.16 (t, 3H, *J* = 7.33 Hz, $C(O)CH_2CH_3$), 2.96 (q, 2H, *J* = 7.33 Hz, $C(O)CH_2CH_3$), 4.91 (bs, 2H, NH_2), 6.17 (dd, 1H, *J* = 3.12 Hz and *J* = 0.85 Hz, 3-H), 6.55 (ddd, 1H, *J* = 8.74 Hz, *J* = 2.13 Hz and *J* = 0.33 Hz, 6-H), 6.70 (dd, 1H, *J* = 2.13 Hz and *J* = 0.61 Hz, 4-H), 7.21 (d, 1H, *J* = 3.12 Hz, 2-H), 7.23 ppm (dt, 1H, *J* = 8.74 Hz and *J* = 0.85 Hz, 7-H); ^{13}C NMR (101 MHz, DMSO-d_6) δ = 9.36 ($C(O)CH_2CH_3$), 28.45 ($C(O)CH_2CH_3$), 100.29 (3-C), 104.03 (4-C), 110.31 (7-C), 112.33 (6-C), 128.44 (2-C), 129.70 (3a-C), 129.75 (7a-C), 142.19 (5-C), 174.80 ppm (NC(O)). HRMS (ESI-MS, 140 eV): *m/z* [M + H^+] calculated for $C_{11}H_{13}N_2O^+$, 189.2332; found, 189.2388.

Cyclopropyl(5-amino-1*H*-indol-1-yl)methanone (3f)

Compound **3f** was prepared as for compound **3e** by reacting 0.500 g of of 5-nitroindole **2f** (2.15 mmol), 2.9 g of $SnCl_2 \cdot 2H_2O$ (12.85 mmol), and 30 mL of methanol to yield 0.205 g of a pearly white solid. Yield 47%. R_f = 0.70 (*n*-hexane/ethyl acetate, 2:8); ^{1}H NMR (300 MHz, DMSO-d_6) δ = 1.03 (m, 4H, CH_2-CH_2), 2.60 (m, 1H, CH), 4.91 (s, 2H, NH_2), 6.54 (dd, 1H, *J* = 3.62 Hz and *J* = 0.57 Hz, 3-H), 6.57 (dd, 1H, *J* = 8.77 Hz and *J* = 2.09 Hz, 6-H), 6.71 (d, 1H, *J* = 2.09 Hz, 4-H), 7.98 (d, 1H, *J* = 3.24 Hz, 2-H), 8.00 ppm (dd, 1H, *J* = 8.77 Hz and *J* = 0.57 Hz, 7-H); ^{13}C NMR (75 MHz, DMSO-d_6) δ = 15.95 (CH_2CH_2), 28.44 (CH), 101.15 (3-C), 104.33 (4-C), 112.77 (7-C), 113.24 (6-C), 128.06 (2-C), 128.94 (3a-C), 129.74 (7a-C), 142.52 (5-C), 171.61 ppm ($NC(O)CHCH_2CH_2$). HRMS (ESI-MS, 140 eV): *m/z* [M + H^+] calculated for $C_{12}H_{13}N_2O^+$, 201.2439; found, 201.2482.

General Procedure for the Synthesis of Acrylate Derivatives 4a–f and 7f

As a typical procedure, the synthesis of acrylate derivative **4a** is described in detail. In a 100 mL round-bottomed flask, 1.234 g (7.00 mmol) of 3-substituted aminoindole **3a** in 25 mL of absolute ethanol was condensed with 1.82 mL (10.5 mmol; *d* = 1.11 g/mL) of commercial ethyl benzoylacetate and 0.5 mL of glacial acetic acid in the presence of 100 mg of Drierite. The mixture was refluxed for about 24 h, the reaction being monitored by TLC analysis (*n*-hexane/ethyl acetate, 3:7). Even though the reaction was not complete after 24 h, the mixture was cooled and filtered to remove the Drierite; the resulting solution was evaporated to dryness under vacuum and the residue (2.420 g) purified by silica gel chromatography (*d* = 3 cm, *l* = 35 cm, 230–400 mesh, eluent *n*-hexane/ethyl acetate, 3:7) to yield 1.47 g of a semisolid yellow product.

(*E*,*Z*)-Ethyl 3-(1-(2-Hydroxyethyl)-1*H*-indol-5-ylamino)-3-phenylacrylate (4a)

Yield 60%; R_f = 0.58 (*n*-hexane/ethyl acetate, 3:7); ^{1}H NMR (300 MHz, DMSO-d_6) δ = 1.11 (t, 3H, *J* = 7.05 Hz, CH_2CH_3), 3.89 (q, 2H, *J* = 7.05 Hz, CH_2CH_2OH), 4.13 (q, 2H, *J* = 7.05 Hz, CH_2CH_3), 4.61 (t, 2H, *J* = 7.05 Hz, CH_2CH_2OH), 4.83 (s, 1H, CH), 5.15 (t, 1H, *J* = 7.05 Hz, OH), 7.16 (d, 1H, *J* = 3.05 Hz, 3-H), 7.67 (m, 5H, 2′-H, 3′-H, 4′-H, 5′-H, 6′-H), 7.71 (dd, 1H, *J* = 8.77 and *J* = 2.10 Hz, 6-H), 8.02 (d, 1H, *J* = 2.10 Hz, 4-H), 8.07 (d, 1H, *J* = 3.05 Hz, 2-H), 8.13 (d, 1H, *J* = 8.77 Hz, 7-H), 10.25 ppm (s, 1H, NH); ^{13}C NMR (75 MHz, DMSO-d_6) δ = 14.75 ($CHCOOCH_2CH_3$), 46.94 (NCH_2 CH_2 OH), 60.24 ($CHCOOCH_2$ CH_3), 61.56 (NCH_2CH_2OH), 89.44 ($CHCOOCH_2CH_3$), 102.62 (3-C), 110.75 (7-C), 114.73 (4-C), 118.12 (6-C), 127.22 (3a-C), 128.94 (2′-C and 6′-C), 129.44 (5′-C and 3′-C), 129.87 (4′-C), 130.44 (2-C), 132.03 (7a-C), 133.76 (1′-C), 137.42 (5-C), 159.92 (NHCCH), 169.84 ppm ($CHCOOCH_2CH_3$). HRMS (ESI-MS, 140 eV): *m/z* [M + H^+] calculated for $C_{21}H_{23}N_2O_3^+$, 351.4184; found, 351.4194.

(*E*,*Z*)-Ethyl 3-(1-(Cyclopropylmethyl)-1*H*-indol-5-ylamino)-3-(3,4-dimethoxyphenyl)acrylate (4b)

Compound **4b** was prepared as for compound **4a** by reacting 0.500 g (2.68 mmol) of 5-aminoindole **3b**, obtaining after column chromatography 0.387 g of a semisolid product. Yield 87%; R_f = 0.76 and R_f = 0.70 (ethyl acetate); ^{1}H NMR (300 MHz, DMSO-d_6) including NMR signals of both isomers δ = 0.32 (dd, 2H, *J* = 4.95 Hz and *J* = 1.14 Hz, CH_2-CH_2), 0.46 (dd, 2H, *J* = 8.20 Hz and *J* = 1.90 Hz, CH_2-CH_2), 1.17 (t, 3H, *J* = 7.05 Hz, CH_2CH_3), 1.23 (t, 3H, *J* = 7.05 Hz, CH_2CH_3), 1.29 (m, 1H, CH), 3.54 and 3.68 (s, 6H, -OCH_3), 3.81 and 3.85 (s, 6H, -OCH_3), 4.09 (m, 2H, *J* = 6.29 Hz, CH_2CH_3), 4.13 (m, 2H, *J* = 7.05 Hz, CH_2CH_3), 4.88 (s, 1H, CH), 6.10 and 6.25 (dd, 2H, *J* = 2.86 Hz and *J* = 0.76 Hz, *J* = 3.05 Hz, *J* = 0.57 Hz, 3-H), 6.51 (dd, 2H, *J* = 9.15 Hz and *J* = 2.09 Hz, 6-H), 6.64 (dd, 2H, *J* = 8.39 and *J* = 1.90 Hz, 6′-H), 6.82 (d, 1H, *J* = 8.96 Hz, 5′-H), 7.02 (d, 1H, *J* = 0.90 Hz, 2′-H), 7.12 (d, 1H, *J* = 8.58 Hz, 7-H), 7.18 (dd, 2H, *J* = 6.29 Hz and *J* = 3.05 Hz, 4-H), 7.31 and 7.36 (d, 2H, *J* = 8.77 Hz and *J* = 3.05 Hz, 5-H), 7.44 (d, 1H, *J* = 2.09 Hz, 2-H), 7.61 (dd, 1H, *J* = 8.58 Hz and *J* = 2.28 Hz, 6-H), 10.19 ppm (s, 1H, NH); ^{13}C NMR (75 MHz, DMSO-d_6) δ = 8.24 (CH_2CH_2), 13.07 (CH), 14.34 ($CHCOOCH_2CH_3$), 60.24 ($CHCOOCH_2CH_3$), 62.04 (OCH_3), 62.61 (OCH_3), 88.78 ($CHCOOCH_2CH_3$), 101.91 (3-C), 111.77 (7-C), 114.97 (4-C), 115.85 (2′-C), 117.24 (6-C), 119.82 (5′-C), 122.45 (6′-C), 126.92 (3a-C), 130.44 (2-C), 132.03 (7a-C), 135.62 (1′-C), 137.23 (5-C), 160.44 (NHCCH), 163.03 (3′-C), 164.24 (4′-C), 169.84 ppm ($CHCOOCH_2CH_3$). HRMS (ESI-MS, 140 eV): *m/z* [M + H^+] calculated for $C_{25}H_{29}N_2O_4^+$, 421.5082; found, 421.5095.

(*E*,*Z*)-Ethyl 3-(1-(2-Cyanoethyl)-1*H*-indol-5-ylamino)-3-phenylacrylate (4c)

Compound **4c** was prepared as for compound **4a** by reacting 2.148 g (11.60 mmol) of 5-aminoindole derivative **3c** and 3.01 mL (17.7 mmol) of ethyl benzoylacetate, obtaining after column chromatography (*d* = 3 cm, *l* = 30 cm, 230–400 mesh, eluent *n*-hexane/ethyl acetate, 1:1) 2.54 g of a dark red solid. Yield 71%; R_f = 0.72 (*n*-hexane/ethyl acetate, 1:1); ^{1}H NMR (400 MHz, DMSO-d_6) δ = 1.24 (t, 3H, *J* = 6.92 Hz, $CHCOOCH_2CH_3$), 2.97 (t, 2H, *J* = 6.34 Hz, NCH_2CH_2CN), 4.14 (q, 2H, *J* = 6.92 Hz,, $CHCOOCH_2CH_3$), 4.39 (t, 2H, *J* = 6.34 Hz, NCH_2CH_2CN), 4.85 (s, 1H, $CHCOOCH_2CH_3$), 6.28 (dd, 1H, *J* = 3.19 Hz and *J* = 0.69 Hz,

3-H), 6.66 (dd, 1H, *J* = 8.71 Hz and *J* = 2.08 Hz, 6-H), 6.98 (m, 1H, *J* = 2.08 Hz, 4-H), 7.29 (m, 1H, 2-H), 7.29 (m, 1H, 4′-H), 7.35 (m, 1H, 7-H), 7.37 (m, 2H, 2′-H and 6′-H), 7.35 (m, 2H, 3′-H and 5′-H), 10.27 ppm (s, 1H, NH); ^{13}C NMR (101 MHz, DMSO-d_6) δ = 14.94 ($CHCOOCH_2CH_3$), 19.01 (NCH_2CH_2CN), 41.71 (NCH_2CH_2CN), 59.14 ($CHCOOCH_2CH_3$), 89.12 ($CHCOOCH_2CH_3$), 101.68 (3-C), 110.44 (7-C), 115.25 (4-C), 118.75 (6-C), 119.29 (CN), 128.64 (3a-C), 128.89 (2′-C and 6′-C), 128.59 (5′-C and 3′-C), 129.85 (4′-C), 129.87 (2-C), 132.93 (7a-C), 133.06 (1′-C), 136.31 (5-C), 160.50 (NHCCH), 169.79 ppm ($CHCOOCH_2CH_3$). HRMS (ESI-MS, 140 eV): *m/z* [M + H^+] calculated for $C_{22}H_{22}N_3O_2^+$, 360.4284; found, 360.4242.

(*E*,*Z*)-Ethyl 3-(1-((Ethoxycarbonyl)methyl)-1*H*-indol-5-ylamino)-3-phenylacrylate (4d)

Compound **4d** was prepared as for compound **4a** by reacting 0.800 g (3.66 mmol) of 5-aminoindole **3d**, to yield after silica gel column chromatography (*d* = 2.5 cm, *l* = 30 cm, 230–400 mesh, eluent *n*-hexane/ethyl acetate, 1:1) 1.024 g of a semisolid red product. Yield 70%; R_f = 0.54 (*n*-hexane/ethyl acetate, 1:1); ^{1}H NMR (300 MHz, DMSO-d_6) δ = 1.11 (t, 3H, *J* = 7.05 Hz, CH_2CH_3), 1.16 (t, 3H, *J* = 7.05 Hz, CH_2CH_3), 4.01 (q, 2H, *J* = 7.05 Hz, CH_2CH_3), 4.13 (q, 2H, *J* = 7.05 Hz, CH_2CH_3), 4.83 (s, 1H, CH), 4.95 (s, 2H, CH_2) 6.20 (d, 1H, *J* = 3.05 Hz, 3-H), 6.60 (dd, 1H, *J* = 8.77 Hz and *J* = 2.10 Hz, 6-H), 6.97 (d, 1H, *J* = 2.10 Hz, 4-H), 7.30 (m, 7H, 2-H, 7-H, 2′-H, 3′-H, 4′-H, 5′-H, and 6′-H), 10.25 ppm (s, 1H, NH); ^{13} C NMR (75 MHz, DMSO-d_6) δ = 14.33 ($CHCOOCH_2CH_3$), 15.64 ($NCH_2COOCH_2CH_3$), 46.55 ($NCH_2COOCH_2CH_3$), 60.24 ($CHCOOCH_2CH_3$), 61.15 ($NCH_2COOCH_2CH_3$), 88.95($CHCOOCH_2CH_3$), 102.36 (3-C), 110.82 (7-C), 114.46 (4-C), 118.25 (6-C), 127.16 (3a-C), 128.77(2′-C and 6′-C), 129.41 (5′-C and 3′-C), 129.82 (4′-C), 130.11 (2-C), 132.09 (7a-C), 133.24 (1′-C), 137.77 (5-C), 160.14 (NH C CH), 168.88 ($CHCOOCH_2CH_3$), 169.76 ppm ($NCH_2COOCH_2CH_3$);HRMS (ESI-MS, 140 eV): *m/z* [M + H^+] calculated for $C_{23}H_{25}N_2O_4$, 393.4551; found, 393.4577.

(*E*,*Z*)-Ethyl 3-(1-Propionyl-1*H*-indol-5-ylamino)-3-phenylacrylate (4e)

Compound **4e** was prepared as for compound **4a** by reacting 0.240 g (1.28 mmol) of 5-aminoindole **3e** and 0.332 mL of ethyl benzoyl acetate (1.92 mmol, *d* = 1.11 g/mL). An amount of 0.525 g of a crude product was obtained, and this was purified by silica gel column chromatography (*d* = 2 cm, *l* = 15 cm, 230–400 mesh, eluent *n*-hexane/ethyl acetate/toluene, 1:1:1), giving 0.250 g of a semisolid yellow product. Yield 53%; R_f = 0.72 (ethyl acetate/*n*-hexane/toluene, 1:1:1); ^{1}H NMR (400 MHz, DMSO-d_6) δ = 1.16 (t, 3H, *J* = 7.33 Hz, $C(O)CH_2CH_3$), 1.24 (t, 3H, *J* = 6.92 Hz, $COOCH_2CH_3$), 2.96 (q, 2H, *J* = 7.33 Hz, $C(O)CH_2CH_3$), 4.14 (q, 2H, *J* = 6.92 Hz, $COOCH_2CH_3$), 4.85 (s, 1H, CH), 6.28 (dd, 1H, *J* = 3.19 Hz and *J* = 0.69 Hz, 3-H), 6.66 (dd, 1H, *J* = 8.70 Hz and *J* = 2.08 Hz, 6-H), 6.97 (m, 1H, *J* = 2.08 Hz, 4-H), 7.28 (d, 1H, *J* = 3.19 Hz, 2-H), 7.29 (m, 1H, 4′-H), 7.34 (m, 2H, 3′-H and 5′-H), 7.35 (dd, 1H, *J* = 8.70 Hz and *J* = 0.69 Hz, 7-H), 7.37 (m, 2H, 2′-H and 6′-H), 10.26 ppm (bs, 1H, NH); ^{13}C NMR (101 MHz, DMSO-d_6) δ = 9.36 ($C(O)CH_2CH_3$), 14.94 ($COOCH_2CH_3$), 28.45 ($C(O)CH_2CH_3$), 59.14 ($COOCH_2CH_3$), 89.11 (CH), 101.68 (3-C), 110.44 (7-C), 115.25 (4-C), 118.76 (6-C), 128.59 (3′-C and 5′-C), 128.64 (3a-C), 128.89 (2′-C and 6′-C), 129.84 (4′-C), 129.87 (2-C), 132.93 (7a-C), 133.06 (1′-C), 136.31 (5-C),

160.51 (C-CH), 169.79 ($COOCH_2CH_3$), 174.80 ppm ($COCH_2CH_3$). HRMS (ESI-MS, 140 eV): *m/z* [M + H] calculated for $C_{22}H_{23}N_2O_3^+$, 363.4291; found, 363.4273.

(*E*,*Z*)-Ethyl 3-(1-Cyclopropylmethanone-1*H*-indol-5-ylamino)-3-phenylacrylate (4f)

Compound **4f** was prepared as for compound **4a** by reacting 0.750 g (3.74 mmol) of 5-aminoindole derivative **3f** with ethyl benzoylacetate (1.72 mL, 5.61 mmol). An amount of 1.150 g of crude product was obtained, and this was chromatographed on a silica gel column (*d* = 2.5 cm, *l* = 30 cm, 230–400 mesh, eluent ethyl acetate/*n*-hexane, 4:6) yielding 0.694 g of a yellow oil. Yield 49%; R_f = 0.76 (ethyl acetate/*n*-hexane, 4:6); ^{1}H NMR (300 MHz, DMSO-d_6) δ = 1.05 (m, 4H, CH_2CH_2), 1.17 (t, 3H, *J* = 7.05 Hz, CH_2CH_3), 2.64 (m, 1H, CH), 4.13 (q, 2H, *J* = 7.05 Hz, CH_2CH_3), 4.92 (s, 1H, CH), 6.58 (d, 1H, *J* = 3.62 Hz, 3-H), 6.73 (dd, 1H, *J* = 8.84 Hz and *J* = 2.01 Hz, 6-H), 6.99 (d, 1H, *J* = 2.01 Hz, 4-H), 7.32 (m, 3H, 3′-H, 5′-H and 4′-H), 7.94 (m, 2H, *J* = 7.43 Hz, 2′-H and 6′-H), 8.01 (d, 1H, *J* = 8.77 Hz, 7-H), 8.11 (d, 1H, *J* = 3.81 Hz, 2-H), 10.24 ppm (s, 1H, NH); ^{13}C NMR (75 MHz, DMSO-d_6) δ = 14.75 ($CHCOOCH_2CH_3$), 15.36 (CH_2CH_2), 28.44 (CH), 61.04 ($CHCOOCH_2CH_3$), 89.27 ($CHCOOCH_2CH_3$), 102.94 (3-C), 110.35 (7-C), 114.68 (4-C), 118.24 (6-C), 127.36 (3a-C), 128.83 (2′-C and 6′-C), 129.26 (5′-C and 3′-C), 129.65 (4′-C), 130.25 (2-C), 132.25 (7a-C), 133.78 (1′-C), 137.89 (5-C), 160.44 (NHCCH), 169.44 ($CHCOOCH_2CH_3$), 171.91 ppm ($NC(O)CHCH_2CH_2$). HRMS (ESI-MS, 140 eV): *m/z* [M + H^+] calculated for $C_{23}H_{23}N_2O_3^+$, 375.4398; found, 375.4356.

(*E*,*Z*)-Ethyl 3-(1-Cyclopropylmethanone-1*H*-indolin-5-ylamino)-3-phenylacrylate (7f)

Compound **7** was prepared as for compound **4a** by reacting 0.653 g (3.22 mmol) of 5-aminoindole derivative **2f** and 0.836 mL diethyl benzoylacetate (4.83 mmol). An amount of 0.956 g of crude product was obtained, and this was purified by silica gel column chromatography (*d* = 2.5 cm, *l* = 35 cm, 230–400 mesh, eluent ethyl acetate/*n*-hexane, 3:7), giving 0.459 g of a yellow solid. Yield 37%. R_f = 0.79 (ethyl acetate/*n*-hexane, 8:2); mp = 133 °C; ^{1}H NMR (300 MHz, DMSO-d_6) δ = 0.80 (m, 4H, CH_2CH_2), 1.17 (t, 3H, *J* = 6.95 Hz, CH_2CH_3), 2.64 (m, 1H, $CH\text{-}COOCH_2CH_3$), 3.18 (t, 2H, *J* = 7.84 Hz, 3-H_2), 4.13 (q, 2H, *J* = 6.95 Hz, CH_2CH_3), 4.29 (t, 2H, *J* = 7.84 Hz, 2-H_2), 6.73 (dd, 2H, *J* = 8.84 Hz and *J* = 2.01 Hz, 6-H), 6.99 (d, 1H, *J* = 2.01 Hz, 4-H), 7.32 (m, 3H, 3′-H, 5′-H and 4′-H), 7.94 (m, 2H, 2′-H and 6′-H), 8.01 (d, 1H, *J* = 8.84 Hz, 7-H), 10.25 ppm (bs, 1H, NH); ^{13}C NMR (75 MHz, DMSO-d_6) δ = 8.44 (CH_2CH_2), 13.96 (CH), 14.26 ($CHCOOCH_2CH_3$), 28.02 (3-C), 48.47 (2-C), 60.84 ($CHCOOCH_2CH_3$), 89.72 ($CHCOOCH_2CH_3$), 110.26 (7-C), 114.75 (4-C), 118.23 (6-C), 127.75 (3a-C), 128.34 (2′-C and 6′-C), 129.34 (5′-C and 3′-C), 129.75 (4′-C), 132.11 (7a-C), 133.87 (1′-C), 137.23 (5-C), 160.86 (NHCCH), 170.07 ($CHCOOCH_2CH_3$), 172.51 ppm ($NC(O)CHCH_2CH_2$). HRMS (ESI-MS, 140 eV): *m/z* [M + H] $^+$ calculated for $C_{23}H_{25}N_2O_3^+$, 377.4557; found, 377.4547.

General Procedure for the Synthesis of Phenylpyrrolo-quinolinones 5a–f and 8f

As a typical procedure, the synthesis of the phenylpyrroloquinolinone derivative **5a** is described in detail. In a two-necked round-bottomed flask, 50 mL of diphenyl ether was heated to boiling. An amount of 1.47 g (4.2 mmol) of acrylate derivative **4a** was then added portionwise, and the resulting mixture was refluxed for 15 min. After cooling to room

temperature, an amount of 25 mL of diethyl ether was added, and the mixture was left for 12 h. Then the separated precipitate was collected by filtration and washed many times with diethyl ether. The product (0.945 g) was purified by silica gel column chromatography (*d* = 2.5, *l* = 30, 230–400 mesh, eluent ethyl acetate/methanol, 9:1), obtaining 0.511 g of a slightly brown product.

3-(2-Hydroxyethyl)-7-phenyl-3*H*-pyrrolo[3,2-*f*] quinolin-9(6*H*)-one (5a)

Yield 40%; R_f = 0.32 (blue fluorescent spot, dichloromethane/methanol, 9:1); mp = 161 °C; ^{1}H NMR (300 MHz, DMSO-d_6) δ = 3.76 (m, 2H, CH_2CH_2OH), 4.34 (t, 2H, *J* = 5.62 Hz, CH_2CH_2OH), 4.94 (bs, 1H, OH), 6.47 (s, 1H, 8-H), 7.49 (d, 1H, *J* = 2.94 Hz, 2-H), 7.53 (m, 1H, 1-H), 7.58 (m, 4H, 5-H, 3′-H, 4′-H and 5′-H), 7.78 (m, 2H, 2′-H and 6′-H), 7.90 (dd, 1H, *J* = 9.02 Hz and *J* = 0.46 Hz, 4-H), 11.74 ppm (bs, 1H, NH); ^{13}C NMR (75 MHz, DMSO-d_6) δ = 49.00 (CH_2CH_2OH), 61.22 (CH_2CH_2OH), 103.98 (1-C), 108.22 (8-C), 112.83 (5-C), 116.38 (4-C), 117.84 (9a-C), 123.38 (9b-C), 127.80 (6′-C and 2′-C), 129.42 (3′-C and 5′-C), 129.72 (2-C), 130.42 (4′-C), 132.16 (1′-C), 132.18 (3a-C), 137.11 (5a-C), 149.63 (7-C), 178.86 ppm (9-C). IR (ATR ZnSe): ν = 3150, 2900, 2850, 1610, 1470, 1055 cm^{-1}. UV–vis (MeOH): λ_{max} (ε) = 206 (1.435), 270 (1.341), 345 nm (0.642); λ_{min} (ε) = 195 (0.453), 247 (0.600), 314 nm (0.344). HRMS (ESI-MS, 140 eV): *m/z* [M + H$^+$] calculated for $C_{19}H_{17}N_2O_2^+$, 305.1290; found, 305.1298. RP-C18-HPLC: 97.24%, t_R = 10.02 min.

3-(Cyclopropylmethyl)-7-(3,4-dimethoxyphenyl)-3*H*-pyrrolo[3,2-*f*] quinolin-9(6*H*)-one (5b)

Compound **5b** was prepared as for compound **5a** by reacting 1.5 g (3.56 mmol) of dimethoxyphenylacrylate derivative **4b**. An amount of 0.801 g of a rough dark green solid was obtained, and this was chromatographed on a silica gel column (*d* = 2.5 cm, *l* = 30 cm, 230–400 mesh, eluent ethyl acetate) yielding 0.450 g of a green solid. Yield 35%; mp = 291 °C; R_f = 0.83 (blue fluorescent spot, ethyl acetate); ^{1}H NMR (300 MHz, DMSO-d_6) δ = 0.41 (m, 2H, CH_2-CH_2), 0.53 (m, 2H, CH_2-CH_2), 1.26 (m, 1H, CH), 3.85 (s, 3H, -OCH_3), 3.90 (s, 3H, -OCH_3), 4.15 (d, 2H, CH_2), 6.37 (bs, 1H, 8-H), 7.14 (d, 1H, *J* = 8.21 Hz, 5-H), 7.56 (m, 2H, 1-H and 5′-H), 7.86 (m, 3H, 2-H, 2′-H and 6′-H), 7.91 (d, 1H, *J* = 8.92 Hz, 4-H), 11.50 ppm (bs, 1H, NH); ^{13}C NMR (75 MHz, DMSO-d_6) δ = 4.87 (CH_2CH_2), 5.28 (CH_2CH_2), 8.83 ($CHCH_2CH_2$), 56.16 (-OCH_3), 61.52 (-OCH_3), 63.51 (–CH_2-) 102.74 (1-C), 106.44 (8-C), 108.21 (5-C), 112.11 (4-C), 116.81 (9a-C), 124.14 (9b-C), 124.86 (4′-C), 125.43 (3′-C), 125.98 (2′-C), 126.14 (2-C), 130.42 (1′-C), 134.21 (3a-C), 135.15 (5a-C), 147.13 (6′-C), 148.56 (7-C), 153.31 (5′-C), 175.23 ppm (9-C). IR (ATR ZnSe): $\tilde{\nu}$ = 3180, 2950, 2880, 1615, 1490 cm^{-1}. UV–vis (MeOH): λ_{max} (ε) = 221 (0.717), 293 (0.670), 343 nm (0.320); λ_{min} (ε) = 258 (0.226), 318 nm (0.172); fluorescence (MeOH), λ_{exc} = 300 nm, λ_{ems} = 451 nm. HRMS (ESI-MS, 140 eV): *m/z* [M + H$^+$] calculated for $C_{23}H_{23}N_2O_3^+$, 375.1709; found, 375.1715. RP-C18-HPLC: 99.82%, t_R = 12.53 min.

3-(9-Oxo-7-phenyl-6*H*-pyrrolo[3,2-*f*] quinolin-3(9*H*)-yl)-propanenitrile (5c)

Compound **5c** was prepared as for compound **5a** by reacting 2.54 g (7.06 mmol) of phenylacrylate derivative **4c**. An amount of 1.680 g of a yellow solid product was obtained. Yield 76%; R_f = 0.72 (blue fluorescent spot, ethyl acetate/methanol, 8:2); ^{1}H NMR (400 MHz, DMSO-d_6) δ = 3.10 (t, 2H, *J* = 6.51 Hz, NCH_2CH_2CN), 4.63 (t, 2H, *J* = 6.51 Hz,

NCH_2CH_2CN), 6.40 (s, 1H, 8-H), 7.50 (m, 1H, 4′-H), 7.56 (m, 1H, 2-H), 7.57 (m, 2H, 3′-H and 5′-H), 7.60 (m, 1H, 5-H), 7.61 (m, 1H, 1-H), 7.86 (m, 2H, 2′-H and 6′-H), 8.00 (d, 1H, J = 8.64 Hz, 4-H), 11.69 ppm (bs, 1H, NH); ^{13}C NMR (101 MHz, DMSO-d_6) δ = 19.55 (NCH_2CH_2CN), 41.85 (NCH_2CH_2CN), 104.81 (1-C), 108.72 (8-C), 113.06 (5-C), 116.04 (4-C), 118.26 (9a-C), 119.27 (CN), 123.90 (9b-C), 127.83 (2′-C and 6′-C), 129.16 (4′-C), 129.44 (3′-C and 5′-C), 130.51 (2-C), 131.63 (5a-C), 135.00 (7-C), 137.04 (3a-C), 137.04 (1′-C), 178.38 ppm (9-C). IR (KBr): υ = 3424, 2247, 1506 cm^{-1}. UV–vis (MeOH): λ_{max} (ε) = 204 (0.608), 269 (0.378), 336 nm (0.179); λ_{min} (ε) = 245 (0.183), 311 nm (0.101). HRMS (ESI-MS, 140 eV): m/z [M + H$^+$] calculated for $C_{20}H_{16}N_3O^+$, 314.1293; found, 314.1303. RP-C_{18} HPLC: t_R = 11.09 min, 98.18%.

Ethyl 2-(9-Oxo-7-phenyl-6*H*-pyrrolo[3,2-*f*] quinolin-3(9*H*)-yl)acetate (5d)

Compound **5d** was prepared as for compound **5a** by reacting 1.024 g (3.15 mmol) of phenylacrylate derivative **4d**. An amount of 0.634 g of a beige solid was obtained, and this was purified by silica gel column chromatography (d = 2.5, l = 35, 230–400 mesh, eluent ethyl acetate) to yield 0.380 g of a golden beige solid. Yield 30%; mp = 107 °C; R_f = 0.27 (fluorescent blue spot, ethyl acetate); ^{1}H NMR (300 MHz, DMSO-d_6) δ = 1.63 (t, 3H, J = 7.02 Hz, CH_2CH_3), 4.20 (q, 2H, J = 7.02 Hz, CH_2CH_3), 4.95 (s, 2H, CH_2), 6.79 (d, 1H, J = 1.38 Hz, 8-H), 7.87 (d, 1H, J = 3.01 Hz, 1-H), 7.99 (m, 5H, 4′-H, 5′-H, 3′-H, 4-H and 2-H), 8.21 (d, 1H, J = 9.06 Hz, 5-H), 8.26 (m, 2H, 2′-H and 6′-H), 11.66 ppm (bs, 1H, NH); ^{13}C NMR (75 MHz, DMSO-d_6) δ = 14.15 (CH_2CH_3), 61.85 (CH_2CH_3), 68.34 (–CH_2-), 102.71 (1-C), 107.62 (8-C), 111.06 (5-C), 114.04 (4-C), 117.26 (9a-C), 124.17 (9b-C), 128.33 (2′-C and 6′-C), 130.15 (4′-C), 130.84 (3′-C and 5′-C), 134.56 (2-C), 135.67 (5a-C), 138.00 (7-C), 138.54 (3a-C), 139.94 (1′-C), 178.68 ppm (9-C). IR (KBr): ν = 3500, 1650, 1500 cm^{-1}. UV–vis (MeOH): λ_{max} (ε) = 203 (0.700), 265 (0.840), 339 nm (0.360), λ_{min} (ε) = 246 (0.650), 314 nm (0.250). HRMS (ESI-MS, 140 eV): m/z [M + H$^+$] calculated for $C_{21}H_{19}N_2O_3^+$, 347.1396; found, 347.1372. RP-C18-HPLC: 98.84%, t_R = 10.07 min.

7-Phenyl-3-propionyl-3*H*-pyrrolo[3,2-*f*] quinolin-9(6*H*)-one (5e)

Compound **5e** was prepared as for compound **5a** by reacting 0.250 g (0.689 mmol) of phenylacrylate derivative **4e**. An amount of 0.130 g of a solid product was obtained, and this was recrystallized from methanol giving 0.065 g of a slightly brown solid. Yield 30%; mp = 289 °C (with decomposition); R_f = 0.73 (blue fluorescent spot, ethyl acetate/methanol, 8:2); ^{1}H NMR (400 MHz, DMSO-d_6) δ = 1.21 (t, 3H, J = 7.23 Hz, $C(O)CH_2CH_3$), 3.15 (q, 2H, J = 7.23 Hz, CH_2), 6.42 (s, 1H, 8-H), 7.59 (m, 3H, 3′-H, 4′-H and 5′-H), 7.75 (d, 1H, J = 9.06 Hz, 5-H), 7.84 (m, 1H, 1-H), 7.86 (m, 2H, 2′-Hand6′-H), 8.03 (d, 1H, J = 3.61 Hz, 2-H), 8.69 (d, 1H, J = 9.06 Hz, 4-H), 11.84 ppm (bs, 1H, NH); ^{13}C NMR (101 MHz, DMSO-d_6) δ = 9.03 (CH_2CH_3), 28.87 (CH_2CH_3), 109.01 (8-C), 109.93 (1-C), 116.03 (5-C), 117.78 (9a-C), 120.77 (4-C), 126.75 (9b-C), 127.43 (2-C), 127.91 (2′-C and 6′-C), 129.45 (3′-C and 5′-C), 130.73 (4′-C), 131.03 (3a-C), 134.77 (1′-C), 138.60 (5a-C), 149.10 (7-C), 173.03 ($C(O)CH_2CH_3$), 178.51 ppm (9-C). IR (ATR ZnSe): ν = 2937, 1701, 1627, 1461 cm^{-1}. UV–vis (MeOH): λ_{max} (ε) = 203 (0.374), 272 (0.445), 326 nm (0.165); λ_{min} (ε)= 243 (0.183), 306 nm (0.112); fluorescence (MeOH), λ_{exc} = 272 nm, λ_{ems} = 413 nm. HRMS (ESI-MS,

140 eV): *m/z* [M + H^+] calculated for $C_{20}H_{17}N_2O_2^+$, 317.1290; found, 317.1301. RP-C18-HPLC: 97.23%, t_R = 12.97 min.

3-(Cyclopropylmethanone)-7-phenyl-H-pyrrolo[3,2-*f*]-quinolin-9(6*H*)-one (5f)

Compound **5f** was prepared as for compound **5a** by reacting 0.650 g (2.13 mmol) of phenylacrylate derivative **4f**. An amount of 0.430 g of a solid product was obtained, and this was recrystallized from ethyl acetate giving 0.266 g of a gray solid. Yield 46%; mp = 298 °C; R_f = 0.62 (chloroform/methanol, 9:1); ^{1}H NMR (300 MHz, DMSO-d_6) δ = 1.15 (m, 4H, CH_2CH_2), 2.79 (m, 1H, CH), 6.41 (s, 1H, 8-H), 7.71 (m, 3H, 3′-H, 4′-H and 5′-H), 7.83 (d, 1H, *J* = 3.46 Hz, 1-H), 7.97 (m, 3H, 5-H, 2′-H, 6′-H), 8.44 (d, 1H, *J* = 3.46 Hz, 2-H), 8.65 (d, 1H, *J* = 8.82 Hz, 4-H), 11.94 ppm (bs, 1H, NH); ^{13}C NMR (75 MHz, DMSO-d_6) δ = 12.45 (CH_2CH_2), 13.05 (CH_2CH_2), 107.94 (8-C), 108.75 (1-C), 115.54 (5-C), 116.40 (9a-C), 119.65 (4-C), 125.65 (9b-C), 126.71 (2-C), 127.15 (2′-C and 6′-C), 128.32 (3′-C and 5′-C), 129.50 (4′-C), 130.83 (3a-C), 132.91 (1′-C), 137.56 (5a-C), 148.40 (7-C), 172.44 ($C(O)CHCH_2CH_2$), 177.31 ppm (9-C). IR (ATR ZnSe): υ = 3350, 3085, 2940, 1724, 1654, 1455 cm^{-1}. UV–vis (MeOH): λ_{max} (ε) = 203 (0.748), 274 (0.880), 325 nm (0.340); λ_{min} (ε)= 243 (0.122), 306 nm (0.168); fluorescence (MeOH), λ_{exc} = 300 nm, λ_{ems} = 412 nm. HRMS (ESI-MS, 140 eV): *m/z* [M + H^+] calculated for $C_{21}H_{17}N_2O_2^+$, 329.1290; found, 329.1297. RP-C_{18} HPLC: t_R = 12.93 min, 98.13%.

3-(Cyclopropylmethanone)-2,3-dihydro-7-phenyl-1*H*-pyrrolo[3,2-*f*] quinolin-9(6*H*)-one (8f)

Compound **8f** was prepared as for compound **5a** by reacting 0.350 g (0.94 mmol) of phenylacrylate derivative **7f**. An amount of 0.202 g of a yellow solid product was obtained, and this was purified by silica gel column chromatography (*d* = 2.5, *l* = 30, 230–400 mesh, eluent ethyl acetate/methanol, 8:2) yielding 0.120 g of a slightly yellow solid. Yield 30%; mp = 317 °C (with decomposition); R_f = 0.67 (blue fluorescent spot, ethyl acetate/methanol, 8:2); ^{1}H NMR (400 MHz, DMSO-d_6) δ = 0.88 (m, 4H, CH_2CH_2), 1.95 (m, 1H, CH), 3.77 (t, 2H, *J* = 8.34 Hz, 1-H_2), 4.36 (t, 2H, *J* = 8.34 Hz, 2-H_2), 6.22 (d, 1H, *J* = 1.82 Hz, 8-H), 7.58 (m, 4H, 5-H, 3′-H, 4′-H, and 5′-H), 7.81 (m, 2H, 2′-H and 6′-H), 8.41 (d, 1H, *J* = 8.49 Hz, 4-H), 11.75 ppm (bs, 1H, NH); ^{13}C NMR (101 MHz, DMSO-d_6) δ = 8.25 (CH_2CH_2), 13.68 (CH), 29.69 (1-C), 49.06 (2-C), 107.58 (8-C), 118.08 (5-C), 120.78 (4-C), 122.38 (9a-C), 127.68 (2′-C and 6′-C), 129.43 (3′-C and 5′-C), 130.27 (9b-C), 130.83 (4-C), 134.57 (1′-C), 138.00 (3a-C), 139.96 (5a-C), 149.63 (7-C), 171.43 ($C(O)CHCH_2CH_2$), 178.86 (9-C). IR (ATR ZnSe): υ = 2960, 2920, 1630, 1590, 1440 cm^{-1}. UV–vis (MeOH): λ_{max} (ε) = 204 (0.992), 279 (1.557), 352 nm (0.281); λ_{min} (ε)= 195 (0.322), 237 (0.443), 336 nm (0.225); fluorescence (MeOH), λ_{exc} = 277 nm, λ_{ems} = 460 nm. HRMS (ESI-MS, 140 eV): *m/z* [M + H^+] calculated for $C_{21}H_{19}N_2O_2^+$, 331.1441; found, 331.1423. RP-C_{18} HPLC: t_R = 11.56 min, 96.33%.

General Procedure for Synthesis of 9-Alkoxyphenylpyrrolo-quinolinones 9–11

As a typical procedure, the synthesis of 9-methoxyl derivative 9 is described in detail. Into a two-necked 50 mL flask 0.0625 g (2.60 mmol) of NaH 60% was placed and washed three times with toluene and finally suspended in 15 mL of anhydrous THF under a nitrogen atmosphere. Then, to the cooled suspension, 0.150 g (0.520 mmol) of starting material 19

(MG 2474)[7] was added. The reaction mixture changed from yellow to slightly brown while developing white fumes (hydrogen) and was stirred for 45 min. Next, 0.01 mL (1.56 mmol, d = 2.28 g/mL) of CH_3I in 1 mL of anhydrous THF was introduced, and the resulting mixture was stirred at room temperature. The progress of the reaction was monitored by TLC analysis (ethyl acetate/methanol, 9:1). After 12 h, the reaction mixture was treated with 20 mL of water, neutralized with 3 N HCl and extracted with ethyl acetate (3 × 50 mL). The combined extracts were dried with anhydrous Na_2SO_4, and the solvent was removed on a rotavapor to yield 0.156 g of a dark dense liquid. The crude reaction product was purified by silica gel column chromatography (d = 2.5, l = 25 cm, 230–400 mesh, eluent ethyl acetate/methanol, 9:1) to yield 0.100 g of a white solid.

3-Ethyl-9-methoxy-7-phenyl-3*H*-pyrrolo[3,2-*f*] quinoline (9)

Yield 64%; mp = 248 °C; R_f = 0.88 (green fluorescent spot, ethyl acetate/methanol, 9:1); ^{1}H NMR (400 MHz, DMSO-d_6) δ = 1.42 (t, 3H, J = 7.21 Hz, CH_2CH_3), 4.23 (s, 3H, OCH_3), 4.37 (q, 2H, J = 7.21 Hz, CH_2CH_3), 7.20 (dd, 1H, J = 3.00 and J = 0.69 Hz), 7.44 (m, 1H, 4′-H), 7.54 (m, 3H, 2-H, 3′-H, 5′-H), 7.60 (s, 1H, 8-H), 7.74 (d, 1H, J = 9.08 Hz, 5-H), 7.96 (dd, 1H, J = 9.08 Hz and J = 0.69 Hz, 4-H), 8.29 ppm (dd, 2H, J = 8.34 Hz and J = 1.31 Hz, 6′-H, 2′-H); ^{13}C NMR (75 MHz, DMSO-d_6) δ = 15.48 (CH_2CH_3), 40.14 (CH_2CH_3), 55.39 (OCH_3), 104.38 (C-1), 113.35 (C-8), 114.75 (C-9a), 118.09 (C-4), 119.08 (C-5), 122.11 (C-9b), 126.28 (C-2), 126.48 (C-2′ and C-6′), 128.28 (C-3′ and C-5′), 130.93 (C-4′), 139.16 (C-3a), 139.45 (C-1′), 145.33 (C-5a), 153.17 (C-7), 162.66 ppm (C-9). UV–vis (MeOH): λ_{max}= 218 (0.984), 265 (0.525), 351 nm (0.367); λ_{min}= 247 (0.634), 310 nm (0.145). HRMS (ESI-MS, 140 eV): m/z $[M + H]^+$ calculated for $C_{20}H_{19}N_2O^+$, 303.1497; found, 303.1491. RP-C18-HPLC: 99.02%, t_R = 15.93 min.

3-Ethyl-7-phenyl-9-butoxy-3*H*-pyrrolo[3,2-*f*] quinoline (10)

Compound **10** was prepared as for compound **9** by reacting 0.300 g (1.04 mmol) of compound **22** dissolved in 5 mL of anhydrous DMF and 0.17 mL (1.56 mmol; d = 1.27 g/mL) of BrC_4H_9 in 1 mL of di-DMF. An amount of 0.348 g of a dark brown solid was obtained, and this was recrystallized from methanol giving 0.259 g of a slightly brown solid. Yield 72%; mp = 120 °C; R_f = 0.87 (green fluorescent spot, ethyl acetate/methanol, 8:2); ^{1}H NMR (300 MHz, DMSO-d_6) δ = 1.03 (t, 3H, J = 7.52 Hz, $CH_2CH_2CH_2CH_3$), 1.41 (t, 3H, J = 7.23 Hz, CH_2CH_3), 1.63 (sextet, 2H, J = 7.52 Hz, $CH_2CH_2CH_2CH_3$), 1.98 (quintuplet, 2H, J = 7.52 Hz and J = 6.15 Hz, $CH_2CH_2CH_2CH_3$), 4.34 (q, 2H, J = 7.23 Hz, CH_2CH_3), 4.44 (t, 2H, J = 6.15 Hz, $CH_2CH_2CH_2CH_3$), 7.23 (d, 1H, J = 2.81 Hz, 1-H), 7.46 (m, 1H, 4′-H), 7.54 (d, 1H, J = 2.81 Hz, 2-H), 7.54 (m, 3H, 2′-H, 3′-H, 5′-H), 7.60 (s, 1H, 8-H), 7.75 (d, 1H, J = 9.09 Hz, 5-H), 7.94 (d, 1H, J = 9.09 Hz, 4-H), 8.30 ppm (m, 1H, 6′-H); ^{13}C NMR (75 MHz, DMSO-d_6) δ = 14.2 2 ($CH_2CH_2CH_2CH_3$), 16. 46 (CH_2CH_3), 19.54 ($CH_2CH_2CH_2CH_3$), 31.26 ($CH_2CH_2CH_2CH_3$), 41.10 (CH_2CH_3), 68.45 ($CH_2CH_2CH_2CH_3$), 99.25 (C-8), 105.16 (C-1), 114.36 (C-9a), 115.64 (C-4), 120.17 (C-9b), 123.17 (C-4 and C-5), 127.29 (C-2′ and C-6′), 129.01 (C-3′ and C-5′), 129.21 (C-4′), 131.94 (C-3a), 140.19 (C-1′), 146.41 (C-5a), 154.14 (C-7), 162.96 ppm (C-9). UV–vis (MeOH): λ_{max} (ε) = 210 (1.011), 239 (0.743), 284 nm (1.610); λ_{min} (ε)= 229 (0.663), 248 nm (0.591). IR (ATR ZnSe): 2953–2869 (CH_2, CH_3), 1524–1469 (C=C), 1230 (C–O) cm^{-1}; fluorescence (MeOH), λ_{exc} = 284 nm, λ_{em} = 514.92 nm. HRMS (ESI-MS, 140 eV): m/z $[M + H]^+$

calculated for $C_{23}H_{25}N_2O^+$, 345.1967; found, 345.1997. RP-C18 HPLC: 99.84%, t_R = 17.60 min.

9-(Benzyloxy)-3-ethyl-7-phenyl-3*H*-pyrrolo[3,2-*f*] quinoline (11)

Compound **11** was prepared as for compound **9** by reacting 0.150 g (0.520 mmol) of compound **22** dissolved in 5 mL of anhydrous DMF and 0.360 g (1.560 mmol) of 4-nitrobenzylbromide dissolved in 2–3 mL of anhydrous DMF. An amount of 0.164 g of a dark brown solid product was obtained, and this was purified by silica gel column chromatography (*d* = 2.5, *l* = 25 cm, 230–400 mesh, eluent ethyl acetate/methanol, 9:1) giving 0.132 g of a brown solid. Yield 74%; mp = 131–134 °C; R_f = 0.76 (green fluorescent spot, ethyl acetate/methanol, 8:2); ^{1}H NMR (300 MHz, $CDCl_3$) δ = 1.50 (t, 3H, *J* = 7.25 Hz, CH_2CH_3), 4.25 (q, 2H, *J* = 7.31 Hz, CH_2CH_3), 5.96 (s, 2H, -CH_2-), 7.15 (d, 1H, *J* = 3.01 Hz, 1-H), 7.23 (d, 1H, *J* = 3.02 Hz, 2-H), 7.51 (m, 3H, 3′-H, 4′-H, and 5′-H), 7.61 (d, 2H, *J* = 8.55 Hz, 2″-H and 6″-H), 7.84 (d, 1H, *J* = 9.09 Hz, 5-H), 7.93 (s, 1H, 8-H), 8.15 (d, 1H, *J* = 9.03 Hz, 4-H), 8.27 (dd, 2H, *J* = 7.17 Hz and *J* = 3.23 Hz, 2′-H and 6′-H), 8.35 ppm (m, 3H, *J* = 8.77 Hz, 3″-H, 4″-H, and 5″-H); ^{13}C NMR (75 MHz, $CDCl_3$) δ = 15.31 (CH_2CH_3), 41.04 (CH_2CH_3), 45.96 (–CH_2-), 104.05 (C-1), 110.02 (C-8), 115.18 (C-4), 115.52 (C-5), 118.45 (C-9a), 126.10 (C-9b), 127.96 (C-2), 128.39 (C-2″ and C-6″), 128.43 (C-2′ and C-6′), 128.53 (C-3″ and C-5″), 128.75 (C-3′ and C-5′), 129.23 (C-4″), 129.54 (C-4′), 131.97 (C-3a), 134.28 (C-1″), 134.81 (C-1′), 152.33 (C-5a), 154.26 (C-7), 164.72 (C-9), 170.94 ppm (–COO). UV–vis (MeOH): λ_{max} (ε) = 205 (0.925), 239 (0.524), 281 nm (0.295); λ_{min} (ε) = 231 (0.628), 247 nm (0.263). HRMS (ESI-MS, 140 eV): *m/z* $[M + H]^+$ calculated for $C_{26}H_{23}N_2O^+$ = 379.1810; found, 379.1805. RP-C18-HPLC: 96.54%, t_R = 16.74 min.

Synthesis of Benzyl 3-Ethyl-7-phenyl-3*H*-pyrrolo[3,2-*f*]-quinolin-9-ylcarbonate (12)

Into a two-necked 50 mL flask 0.0625 g (2.60 mmol) of NaH 60% was placed and washed at least three times with toluene and finally suspended in 15 mL of anhydrous THF under a nitrogen atmosphere. Then, to the ice-bath cooled suspension, 0.150 g (0.520 mmol) of the starting material **19**[7] was added. The reaction mixture changed from yellow to slightly brown while developing white fumes (hydrogen) and was stirred for 45 min. Next, 0.15 mL (1.04 mmol, *d* = 1.195 g/(mL) of benzylchloroformate in 2 mL of anhydrous THF was introduced, and the mixture was stirred at 0 °C. The progress of the reaction was monitored by TLC analysis (ethyl acetate/methanol, 9:1). After 3 h, the reaction mixture was treated with 15 mL of water, neutralized with 3 N HCl, and extracted with ethyl acetate (3 × 50 mL). The combined extracts were dried with anhydrous Na_2SO_4, and the solvent was removed on a rotavapor to yield a dark yellow semisolid residue that was recrystallized from methanol giving 0.212 g of a yellow solid. Yield 96%; mp = 215–218 °C; R_f = 0.89 (blue fluorescent spot, ethyl acetate/methanol, 9:1); ^{1}H NMR (300 MHz, $CDCl_3$) δ = 1.53 (t, 3H, *J* = 7.30 Hz, CH_2CH_3), 4.31 (q, 2H, *J* = 7.31 Hz, CH_2CH_3), 5.40 (s, 2H, CH_2-Benz), 7.13 (d, 1H, *J* = 3.05 Hz, 1-H), 7.23 (d, 1H, *J* = 3.06 Hz, 2-H), 7.40 (m, 3H, 3″-H, 4″-H, and 5″-H), 7.46 (d, 2H, *J* = 8.57 Hz, 6″-H and 2″-H), 7.51 (m, 3H, 3′-H, 4′-H, and 5′-H), 7.80 (d, 1H, *J* = 8.02 Hz, 5-H), 7.94 (s, 1H, 8-H), 8.05 (d, 1H, *J* = 8.05 Hz, 4-H), 8.18 ppm (m, 2H, *J* = 7.19 Hz and *J* = 3.21 Hz, 6′-H and 2′-H); ^{13}C NMR (75 MHz, $CDCl_3$) δ = 15.62 (CH_2CH_3), 41.08 (CH_2CH_3), 69.37 (CH_2-Benz), 104.05 (C-1), 110.02 (C-8), 115.18 (C-4), 115.52 (C-5), 118.45 (C-9a), 126.10 (C-9b), 127.09 (C-2), 127.96 (C-2″ and C-6″), 128.18 (C-2′

and C-6′), 128.22 (C-3″ and C-5″), 128.27 (C-3′ and C-5′), 129.39 (C-4′), 129.43 (C-4″), 131.97 (C-3a), 134.28 (C-1″), 134.81 (C-1′), 154.26 (C-5a), 154.37 (C-7), 164.72 (C-9), 178.24 ppm (-OCOO-). UV–vis (MeOH): λ_{max} (ε) = 207 (0.458), 284 (0.273), 339 nm (0.101); λ_{min} (ε) = 250 (0.317), 316 nm (0.082). HRMS (ESI-MS, 140 eV): *m/z* $[M + H]^+$ calculated for $C_{27}H_{23}N_2O_3^+$, 423.1709; found, 423.1705. RP-C18-HPLC: 98.52%, t_R = 17.04 min.

3-Ethyl-6-methyl-7-phenyl-3*H*-pyrrolo[3,2-*f*] quinolin-9(6*H*)-one (13)

In a 100 mL flask, 0.175 g (0.58 mmol) of 9-methoxy-3-ethyl-7-phenyl-3*H*-pyrrolo[3,2-*f*] quinoline (**9**) was dissolved in 3 mL of CH_3I. The solution was maintained at reflux for 12 h, and the reaction was monitored by TLC (ethyl acetate/methanol, 8:2) until the starting material 9 disappeared and a new yellow fluorescent spot appeared. Then, 5 mL of 1.5 M NaOH in water was added to the reaction mixture and heating at reflux resumed for 2 h. After cooling, the mixture was extracted with ethyl acetate (4 × 50 mL), and the combined extracts were dried with sodium sulfate and filtered. The solvent was evaporated, giving 0.031 g of a pure yellow solid. Yield 18%; R_f = 0.86 (blue fluorescent spot, ethyl acetate/methanol, 8:2); ^{1}H NMR (400 MHz, DMSO-d_6) δ = 1.42 (t, 3H, *J* = 7.20 Hz, NCH_2CH_3), 3.67 (s, 3H, N(quinoline)-CH_3), 4.37 (q, 2H, *J* = 7.20 Hz, NCH_2CH_3), 6.04 (s, 1H, H-8), 7.57 (m, 1H, H-2), 7.57 (m, 5H, H-2′, H-3′, H-4′, H-5′, H-6′), 7.59 (d, 1H, *J* = 9.35 Hz, H-5), 7.67 (dd, 1H, *J* = 2.92 Hz and *J* = 0.72 Hz, H-1), 8.00 ppm (dd, 1H, *J* = 9.35 Hz and *J* = 0.70 Hz, H-4); ^{13}C NMR (101 MHz, DMSO-d_6) δ = 16.37 (NCH_2CH_3), 38.69 (N(quinoline)-CH_3), 41.02 (NCH_2CH_3), 104.38 (C-1), 110.96 (C-5), 112.59 (C-8), 115.94 (C-4), 119.63 (C-9a), 124.30 (C-2), 124.30 (C-9b), 129.15 (C-3′ and C-5′), 129.24 (C-2′ and C-6′), 129.45 (C-4′), 131.65 (C-1′), 136.68 (C-5a), 138.05 (C-3a), 177.16 ppm (C-9). IR (KBr): 3447.02 (C=O), 2924.41 (CH_3, CH_2CH_3), 1582.55 (C=C), 1450.86 (CH_3) cm^{-1}. UV–vis (MeOH): λ_{max} (ε) = 351 (0.415), 264 (0.746), 219 nm (0.99); λ_{min} (ε) = 306.35 (0.138), 246 nm (0.467). HRMS (ESI-MS, 140 eV): *m/z* $[M + H^+]$ calculated for $C_{20}H_{19}N_2O^+$, 303.1497; found, 303.1500. RP-C18-HPLC: 98.77%, t_R = 11.49 min.

3-(3-Hydroxypropyl)-7-phenyl-3*H*-pyrrolo[3,2-*f*] quinolin-9(6*H*)-one (14)

Into a 100 mL dry two-necked flask, 0.084 g (2.22 mmol) of $LiAlH_4$ and 15 mL of anhydrous THF were placed. After stirring the suspension for 2–3 min under a nitrogen atmosphere, 0.200 g (0.562 mmol) of pyrroloquinolinone derivative **21** dissolved in 15 mL of anhydrous THF was added and the mixture stirred for 2 h at room temperature under a nitrogen atmosphere. The reaction was monitored by TLC (ethyl acetate/*n*-hexane, 8:2). At the end of the reaction, excess $LiAlH_4$ was deactivated by adding 10 mL of saturated NH_4Cl in water. After filtering the suspension, the filtrate was concentrated to dryness on a rotavapor, yielding a dark brown residue. The latter was treated with water and extracted with ethyl acetate (3 × 50 mL). The combined extracts were washed several times with water and dried with sodium sulfate. The solvent was removed in a rotavapor, giving a dark yellow solid (0.156 g). Finally, the reaction product was purified with a silica gel chromatography column (*d* = 3 cm, *l* = 30 cm, 230–400 mesh, eluent ethyl acetate/*n*-hexane, 8:2) to give 0.123 g of a pale-yellow solid. Yield 70%; R_f = 0.45 (blue fluorescent spot, ethyl acetate/*n*-hexane, 8:2); mp = 213-215 °C; ^{1}H NMR (300 MHz, DMSO-d_6) δ = 1.94 (m, 2H, *J* = 6.51 Hz, $NCH_2CH_2CH_2OH$), 3.38 (t, 2H, *J* = 6.13 Hz, $NCH_2CH_2CH_2OH$), 4.38 (t, 2H, *J*

= 6.89 Hz, $NCH_2CH_2CH_2OH$), 5.47 (bs, 1H, OH), 6.70 (s, 1H, 8-H), 7.53 (m, 2H, *J* = 2.92 Hz, 1-H and 2-H), 7.61 (m, 3H, 3′-H, 4′-H and 5′-H), 7.71 (d, 1H, *J* = 8.98 Hz, 5-H), 7.90 (m, 2H, *J* = 7.54 Hz and *J* = 2.31 Hz, 6′-H and 2′-H), 8.01 (d, 1H, *J* = 9.00 Hz, 4-H), 12.46 ppm (bs, 1H, NH); ^{13}C NMR (75 MHz, DMSO-d_6) δ = 33.41 ($NCH_2CH_2CH_2OH$), 42.68 ($NCH_2CH_2CH_2OH$), 57.60 ($NCH_2CH_2CH_2OH$), 103.78 (C-1), 116.56 (C-8), 118.53 (C-4), 122.10 (C-5), 123.36 (C-9a), 127.51 (C-9b), 127.51 (C-2), 128.97 (C-2′ and C-6′), 129.16 (C-3′ and C-5′), 130.23 (C-4′), 131.49 (C-3a), 134.19 (C-1′), 148.29 (C-5a), 156.56 (C-7), 178.74 ppm (C-9). UV– vis (MeOH): λ_{max} (ε) = 205 (0.925), 271 (0.714), 346 nm (0.451); λ_{min} = 248 (0.613), 314 nm (0.514). HRMS (ESI-MS, 140 eV): *m/z* $[M + H]^+$ calculated for $C_{20}H_{19}N_2O_2^+$ = 319.1447; found, 319.1472. RP-C18-HPLC: 98.78%, t_R = 10.25 min.

3-(9-Oxo-7-phenyl-6*H*-pyrrolo[3,2-*f*] quinolin-3(9*H*)-yl)-propanoic Acid (15)

Into a 50 mL two-necked flask, a solution of 0.200 g (0562 mmol) of pyrroloquinolinone derivative **II** (MG 2540) in 15 mL of methanol was placed, and 3 mL of 20% NaOH in water was added. The mixture was stirred at 60–70 °C for about 2 h, and the reaction was monitored by TLC (chloroform/methanol, 9:1). At the end of the reaction, the solution was cooled to room temperature, and the solvent was removed on a rotavapor, yielding a dark yellow solid. The dry residue was treated with water and then extracted with ethyl acetate (2 × 50 mL) to remove unreacted compounds. The aqueous phase was then acidified to pH 3–4 with 37% HCl, and immediately a yellow precipitate formed. The precipitate was collected, washed several times with water, and dried under vacuum to yield 0.157 g of an intensely yellow solid. Yield 85%; R_f = 0.20 (blue fluorescent spot, chloroform/methanol, 9:1); mp = 280 °C; ^{1}H NMR (300 MHz, DMSO-d_6) δ = 2.80 (t, 2H, *J* = 6.76 Hz, NCH_2CH_2COOH), 4.52 (t, 2H, *J* = 6.76 Hz, NCH_2CH_2COOH), 6.54 (s, 1H, 8-H), 7.51 (dd, 2H, *J* = 2.98 Hz, 2-H and 1-H), 7.58 (m, 3H, 3′-H, 4′-H and 5′-H), 7.63 (d, 1H, *J* = 8.96 Hz, 5-H), 7.86 (dd, 2H, *J* = 7.71 Hz and *J* = 2.01 Hz, 6′-H and 2′-H), 7.96 (d, 1H, *J* = 9.00 Hz, 4-H), 12.46 ppm (bs, 1H, NH), (no signal for the carboxylic acid proton); ^{13}C NMR (75 MHz, DMSO-d_6) δ = 34.60 (NCH_2CH_2 COOH), 41.20 (NCH_2CH_2COOH), 103.43 (C-1), 112.40 (C-8), 115.44 (C-5), 122.10 (C-4), 123.24 (C-9a), 127.41 (C-9b), 127.47 (C-2), 128.77 (C-2′ and C-6′), 129.06 (C-3′ and C-5′), 129.97 (C-4′), 130.13 (C-3a), 131.35 (C-1′), 134.22 (C-5a), 147.44 (C-7), 167.35 (COOH), 171.87 ppm (C-9). UV–vis (MeOH): λ_{max} (ε) = 206 (0.981), 271 (0.613), 347 nm (0.451); λ_{min} (ε) = 247 (0.714), 314 nm (0.581). HRMS (ESI-MS, 140 eV): *m/z* $[M + H]^+$ calculated for $C_{20}H_{17}N_2O_3^+$ = 333.1239; found, 333.1265. RP-C18-HPLC: 97.98%, t_R = 9.17 min.

2-(9-Oxo-7-phenyl-6*H*-pyrrolo[3,2-*f*] quinolin-3(9*H*)-yl)acetic Acid (16)

Into a 50 mL two-necked flask, 0.150 g (0.43 mmol) of pyrroloquinolinone derivative **5d** in 8 mL of methanol was place, and 3 mL of 20% NaOH in water was added. The mixture was stirred at 60–70 °C for about 2 h, and the reaction was monitored by TLC (chloroform/methanol, 9:1). At the end of the reaction, the solution was cooled to room temperature, and the solvent was removed on a rotavapor, yielding a greyish-white solid (0.120 g). The residue was treated with water and then extracted with ethyl acetate (2 × 50 mL) to remove unreacted compounds. The aqueous phase was then acidified to pH 3–4 with 37% HCl, and immediately a white precipitate formed. The precipitate was collected, washed several times with water, and dried under vacuum, giving 0.085 g of a white crystalline product. Yield

63%; R_f = 0.18 (chloroform/methanol, 7:3); mp = 273 °C; ^{1}H NMR (300 MHz, DMSO-d_6) δ = 5.67 (s, 2H, CH_2COOH), 6.79 (d, 1H, J = 1.38 Hz, 8-H), 7.87 (d, 1H, J = 3.01 Hz, 1-H), 7.99 (m, 5H, 3′-H, 5′-H, 4′-H, 4-H and 2-H), 8.21 (d, 1H, J = 9.06 Hz, 5-H), 8.26 (m, 2H, 6′-H and 2′-H), 11.66 (bs, 1H, NH), 13.10 ppm (bs, 1H, COOH); ^{13}C NMR (75 MHz, DMSO-d_6) δ = 55.72 (NCH_2COOH), 104.33 (C-1), 113.30 (C-5), 116.34 (C-8), 123.00 (C-4), 124.14 (C-9a), 126.31 (C-9b), 128.31 (C-2), 128.67 (C-2′ and C-6′), 129.67 (C-3′ and C-5′), 130.87 (C-3a), 131.03 (C-4′), 132.15 (C-1′), 135.12 (C-5a), 148.34 (C-7), 168.32 (COOH), 174.12 ppm (C-9). UV–vis (MeOH): λ_{max} (ε) = 226 (0.815), 268 (0.613), 346 nm (0.481); λ_{min} (ε) = 249 (0.724), 315 nm (0.523). HRMS (ESI-MS, 140 eV): *m/z* $[M + H]^+$ calculated for $C_{19}H_{15}N_2O_3^+$ 319.1083, found 319.1060. RP-C18-HPLC: 98.12%, t_R = 8.74 min.

tert-Butyl 3-(9-Oxo-7-phenyl-6*H*-pyrrolo[3,2-*f*] quinolin-3(9*H*)-yl)propylcarbamate (17)

In a 100 mL flask, 0.626 g of pyrroloquinolinone derivative **5c** was dissolved in hot MeOH. The solution was cooled to 0 °C, and 1.310 g (6 mmol) of di-*tert*-butyl dicarbonate and 0.110 g (0.4 mmol) of $CoCl_2 \cdot 6H_2O$ were added. To the resulting suspension 0.757 g (20 mmol), $NaBH_4$ was added portionwise, with development of hydrogen and formation of a black precipitate. The mixture was stirred for 12 h at room temperature, and the formation of the reaction product was monitored by TLC (ethyl acetate/methanol, 8:2). Finally, 0.8 mL (2 mmol, d = 0.955 g/mL) of diethylenetriamine was added, and the mixture was dried on a rotavapor. The resulting clear solid was dissolved in 50 mL of ethyl acetate and the solution washed with a saturated solution of $NaHCO_3$ (3 × 25 mL). The organic phase was dried with anhydrous Na_2SO_4 and evaporated to dryness, yielding 0.644 g of a light brown solid. Yield 77%; R_f = 0.79 (ethyl acetate/methanol, 8:2); ^{1}H NMR (400 MHz, DMSO-d_6) δ = 1.37 (s, 3H, $OC(CH_3)_3$), 1.39 (s, 6H, $OC(CH_3)_3$), 1.89 (quintuplet, 2H, J = 6.942 Hz, $NCH_2CH_2CH_2NHCO$), 2.91 (m, 2H, J = 6.66 Hz and J = 5.88 Hz, $NCH_2CH_2CH_2NHCO$), 4.29 (t, 2H, J = 6.93 Hz, $NCH_2CH_2CH_2NHCO$), 6.38 (d, 1H, J = 1.78 Hz, H-8), 6.97 (t, 1H, J = 5.05 Hz, NHCO), 7.50 (d, 1H, J = 2.87 Hz, H-2), 7.55 (d, 1H, J = 2.77 Hz, H-1), 7.58 (m, 4H, H-3′, H-4′, H-5′, and H-5), 7.85 (m, 2H, H-2′ and H-6′), 7.87 (d, 1H, J = 9.04 Hz, H-4), 11.64 ppm (s, 1H, NH); ^{13}C NMR (101 MHz, DMSO-d_6) δ = 28.68 ($OC(CH_3)_3$), 28.72 ($OC(CH_3)_3$), 31.03 ($NCH_2CH_2CH_2NHCO$), 37.96 ($NCH_2CH_2CH_2NHCO$), 43.84 ($NCH_2CH_2CH_2NHCO$), 104.02 (C-1), 108.63 (C-8), 112.71 (C-5), 118.31 (C-9a), 123.57 (C-9b), 127.81 (C-2′ and C-6′), 129.38 (C-2), 129.43 (C-3′ and C-5′), 130.46 (C-4′), 131.70 (C-3a), 135.04 (C-1′), 136.82 (C-5a), 147.71 (C-7), 156.10 (NHCOO), 178.37 ppm (C-9). IR (KBr): 3461.11 (C=O), 1653 (CONH) cm^{-1}. HRMS (ESI-MS, 140 eV): *m/z* $[M + H]^+$ calculated for $C_{25}H_{28}N_3O_3^+$ = 418.2131; found, 418.2137. RP-C18-HPLC: 96.55%, t_R = 10.76 min.

3-(3-Aminopropyl)-7-phenyl-3*H*-pyrrolo[3,2-*f*] quinolin-9-ol hydrochloride (18)

In a 100 mL flask, 0.644 g (1.54 mmol) of pyrroloquinolinone derivative **17** was dissolved in 55 mL of an ethyl acetate/ethanol 2:1 mixture, and dry HCl gas was bubbled into the solution until a yellow precipitate formed. The mixture was left at 0–4 °C overnight, and the resulting precipitate was collected and dried under vacuum to yield 0.413 g of a powdery beige solid. Yield: 58%; R_f = 0.20 (blue fluorescent spot, chloroform/methanol, 8:2); mp = 194 °C; ^{1}H NMR (400 MHz, DMSO-d_6) δ = 2.16 (quintuplet, 2H, J = 6.84 Hz, $NCH_2CH_2CH_2NH_3^+Cl^-$), 2.77 (m, 2H, $NCH_2CH_2CH_2NH_3^+Cl^-$), 4.58 (t, 2H, J = 6.86 Hz,

NCH_2CH$_2$CH$_2$NH$_3^+$Cl$^-$), 7.42 (dd, 1H, J = 2.99 Hz and J = 0.65 Hz, H-1), 7.67 (s, 1H, H-8), 7.70 (m, 1H, H-4′), 7.71 (m, 2H, H-3′ and H-5′), 7.86 (d, 1H, J = 3.21 Hz, H-2), 8.02 (m, 2H, H-2′ and H-6′), 8.17 (d, 1H, J = 9.19 Hz, H-5), 8.19 (m, 3H, NH_3^+), 8.46 (d, 1H, J = 6.86 Hz, H-4), 14.70 ppm (s, 1H, OH); ^{13}C NMR (101 MHz, DMSO-d_6) δ = 28.94 (NCH$_2$CH$_2$CH$_2$NH$_3^+$Cl$^-$), 36.78 (NCH$_2$CH$_2$CH$_2$NH$_3^+$Cl$^-$), 43.82 (N-CH$_2$CH$_2$CH$_2$NH$_3^+$Cl$^-$), 105.19 (C-8), 105.40 (C-1), 113.22 (C-5), 114.10 (C-9a), 120.13 (C-4), 120.68 (C-9b), 129.05 (C-2′ and C-6′), 129.83 (C-3′ and C-5′), 130.95 (C-2), 132.12 (C-4′), 132.58 (C-3a), 132.61 (C-1′), 137.87 (C-5a), 151.15 (C-7), 169.98 ppm (CO). IR (KBr): 3411.56 (OH), 1618 (C=C) cm^{-1}. UV–vis (MeOH): λ_{max} (ε) = 338 (0.081), 270 (0.162), 204 nm (0.169); λ_{min} (ε) = 312 nm (0.046), 246 nm (0.079); fluorescence (H_2O), λ_{exc} = 215.00 nm, λ_{em} = 430.00 nm. HRMS (ESI-MS, 140 eV): m/z [M + H]$^+$ calculated for $C_{20}H_{20}N_3O^+$ = 318.1606; found, 318.1641, m/(2z) [M + 2H]$_2^+$ calculated for $C_{20}H_{21}N_3O_2^+$ 159.5837; found, 159.5801. RP-C18-HPLC: 99.57%, t_R = 8.96 min.

Biology. Cell Lines and Growth Inhibition Assays

The human cell lines were the following: cervix carcinoma (HeLa), adenocarcinomic alveolar basal epithelial cells (A549), colon adenocarcinoma (HT-29), breast adenocarcinoma (MCF-7), ovarian carcinoma (OVCAR-3), acute T-cell lymphoblastic leukemia (MOLT-3, Jurkat, and CCRF-CEM), chronic myelogenous leukemia cells (K562), B-cell leukemia (RS4;11and SEM), acute myelocytic leukemia cells (MV4;11), and acute monocytic leukemia cells (THP-1). All cell lines were purchased from the American Type Culture Collection. Leukemic cell lines were cultured in RPMI-1640 (Gibco, Milano, Italy), while solid tumor cell lines were cultured in DMEM (Gibco, Milano, Italy). Both media were supplemented with 10% fetal bovine serum (FBS), glutamine (2 mM), penicillin (100 U/mL), and streptomycin (100 μg/mL; all media components were from Life Technologies, Italy) and maintained at 37 °C in a humidified atmosphere with 5% CO_2. The cytotoxic activity of the compounds was determined using a standard MTT based colorimetric assay (Sigma-Aldrich, Milano, Italy). Briefly, cells were seeded at a density of 8×10^3 cells/well in 96-well microtiter plates. After 24 h, cells were exposed to various concentrations of the test compounds. After difierent times, cell survival was determined by the addition of an MTT solution as described previously.[16] The GI_{50} value is defined as the compound concentration required to inhibit cell proliferation by 50%.

PBL from healthy donors were obtained by separation on a Lymphoprep (Fresenius KABI Norge AS) gradient. After extensive washing, cells were resuspended (1.0×10^6 cells/mL) in RPMI-1640 with 10% FBS and incubated overnight. For cytotoxicity evaluations in proliferating PBL cultures, nonadherent cells were resuspended at 5×10^5 cells/mL in growth medium, containing 2.5 μg/mL PHA (Irvine Scientific). Difierent concentrations of the test compounds were added, and viability was determined 72 h later by the MTT test. For cytotoxicity evaluations in resting PBL cultures, nonadherent cells were resuspended (5×10^5 cells/mL) and treated for 72 h with the test compounds, as described above.

HUVECs were prepared from human umbilical cord veins, as previously described.[29] The adherent cells were maintained in M200 medium supplemented with low serum growth supplement containing FBS, hydrocortisone, human epithelial growth factor (hEGF), basic

fibroblast growth factor (bFGF), heparin, gentamycin/amphotericin (Life Technologies, Monza, Italy). Once confluent, the cells were detached by trypsin–EDTA solution and used in experiments from the first to sixth passages.

Effects on Tubulin Polymerization and on Colchicine Binding to Tubulin

To evaluate the effect of the compounds on tubulin assembly in vitro,[17] varying concentrations of compounds were preincubated with 10 μM bovine brain tubulin in glutamate buffer at 30 °C and then cooled to 0 °C. After addition of 0.4 mM GTP, the mixtures were transferred to 0 °C cuvettes in a recording spectrophotometer and warmed to 30 °C. Tubulin assembly was followed turbidimetrically at 350 nm. The IC_{50} was defined as the compound concentration that inhibited the extent of assembly by 50% after a 20 min incubation. The ability of the test compounds to inhibit colchicine binding to tubulin was measured as described[19] except that the reaction mixtures contained 1 μM tubulin, 5 μM [^{3}H]colchicine, and 5 μM test compound.

Analysis of Cell Cycle Distribution

5×10^5 cells in exponential growth were treated with difierent concentrations of test compound for difierent times. After the incubation, cells were collected, centrifuged, and fixed with ice-cold ethanol (70%) and stained with PI as described previously.[45]

Externalization of PS

Surface exposure of PS on apoptotic cells was measured by flow cytometry with a Coulter Cytomics FC500 (Beckmann Coulter, USA) instrument by adding annexin-V-FITC and PI to cells according to the manufacturer′s instructions (annexin-V Fluos, Roche Diagnostic, Monza, Italy).

Western Blot Analysis

Cells were treated with test compounds and, after difierent times, collected, centrifuged, and washed with ice cold phosphate buffered saline. The pellet was then resuspended in lysis buffer as described.[25] The protein concentration in the supernatant was determined using the BCA protein assay (Pierce, Milano, Italy). Equal amounts of protein (10–20 μg) were resolved using SDS–PAGE gel electrophoresis (Criterion precast Tris-HCl gel, Biorad Laboratories, Milano, Italy) and transferred to PVDF Hybond-p membranes (GE Healthcare, Milano, Italy). Membranes were blocked with 2% ECL-blocking solution (GE Healthcare, Milano, Italy) for 2 h, with rotation at room temperature. Membranes were then incubated with primary antibodies against Bcl-2, p53, PARP, procaspase-9, procaspase-8, procaspase-2, Mcl-1, Bcl-XL (Cell Signaling, Milano, Italy), β-actin (Sigma-Aldrich, Milano, Italy), and caspase-3 (Novus Biologicals, Milano, Italy) overnight. Membranes were next incubated with peroxidase-conjugated secondary antibodies (Invitrogen, Milano, Italy) for 60 min. All membranes were visualized using ECL Select (GE Healthcare, Milano, Italy) and exposed to Hyperfilm MP (GE Healthcare, Milano, Italy). To ensure equal protein loading, each membrane was stripped and reprobed with anti-β-actin antibody.

Drug Combination Studies

Cell proliferation was assessed by the MTT assay after treatment. Equal concentrations of cells were plated in triplicate in a 96-well plate and treated for 48 h using scalar dilutions of **5f**, combined with cytarabine (Aractyn, Pfizer), daunorubicin (Pfizer), and dexamethasone (Sigma-Aldrich) at fixed combination ratios. The effectiveness of various drug combinations was analyzed by the Calcusyn, version 2.1 software (Biosoft). The combination index (CI) was calculated according to the Chou–Talalay method. A combination index of 1 indicates an additive effect of the two drugs. Combination index values less than 1 indicate synergy, and combination index values greater than 1 indicate antagonism.

Molecular Docking Simulations

Target Structures—The three-dimensional structures of tubulin in complex with colchicine as well as all selected protein kinases were retrieved from the Protein Data Bank (www.rcsb.org).[21] The collected PDB structures are summarized in Table 2 in Supporting Information.

The assessment of crystallographic structure quality has been performed with the Structure Preparation tool of the Molecular Operation Environment (MOE, version 2014.09) program.[46] Critical structural issues (such as missing or poorly resolved atomic data, anomalous topological properties present in amino acids units as well as anomalous bonding patterns of non amino acids units) were fixed when necessary. Hydrogen atoms were added and their appropriate protonation state was fixed using the Protonate3D tool as implemented in the MOE program. To minimize contacts between hydrogen atoms, the structures were subjected to Amber99 force field[47] minimization until the rms of the conjugate gradient was <0.1 kcal mol^{-1} $Å^{-1}$, keeping the heavy atoms fixed at their crystallographic positions.

Molecular Docking Protocol—All 3-substituted 7-PPyQs were built using the “Builder” module of MOE, and each compound was docked into the presumptive binding sites (colchicine or ATP binding sites) using flexible MOE-Dock methodology. The purpose of MOE-Dock is to search for favorable binding configurations between a small, flexible ligand and a rigid macromolecular target. Searching is conducted within a user-specified 3D docking box, using the “Tabu search”[48] protocol and the MMFF94 force field.[49] Charges for ligands were imported from the MOPAC program[50] output files. MOE-Dock performs a user-specified number of independent docking runs (50 in the present case) and writes the resulting conformations and their energies to a molecular database file. The resulting ligand/protein complexes were subjected to MMFF94 all-atom energy minimization until the rms of conjugate gradient was <0.1 kcal mol^{-1} $Å^{-1}$. GB/SA approximation[51] has been used to model the electrostatic contribution to the free energy of solvation in a continuum solvent model. The interaction energy values were calculated as the energy of the complex minus the energy of the ligand minus the energy of the protein:

$$\Delta E_{inter} = E_{complex} - (E_L + E_{protein})$$

Supplementary Material

Refer to Web version on PubMed Central for supplementary material.

ACKNOWLEDGMENTS

The synthetic work coordinated by M.G.F. was carried out with financial support from the University of Padova, Italy, and the Italian Ministry for University and Research (MIUR), Rome, Italy. The molecular modeling work coordinated by S.M. was carried out with financial support from the University of Padova, Italy, and the Italian Ministry for University and Research (MIUR), Rome, Italy. S.M. is also very grateful to the Chemical Computing Group for its scientific and technical partnership. G.V., R.B. and G.B. thank the Fondazione Cariparo by the "Progetto Ricerca Pediatrica". The content is solely the responsibility of the authors and does not necessarily reffect the official views of the National Institutes of Health.

ABBREVIATIONS USED

PPyQ	phenylpyrroloquinolinone
CA-4	combretastatin A-4
PyQ	3H-pyrrolo[3,2-*f*] quinolin-9-one
ATR	attenuated total reffectance
MOE	Molecular Operating Environment
FBS	fetal bovine serum
PI	propidium iodide
PS	phosphatidylserine
HUVEC	human umbilical vein endothelial cell
PBL	peripheral blood lymphocyte
MTT	3-(4,5-dimethylthiazol-2-yl)-2,5-diphenyltetrazolium bromide

REFERENCES

1. Siegel R, Ma J, Zou Z, Jemal A. Cancer statistics, 2014. Ca-Cancer J. Clin. 2014; 64:9–29. [PubMed: 24399786]
2. Shuttleworth SJ, Silva FA, Cecil ARL, Tomassi CD, Hill TJ, Raynaud FI, Clarke PA, Workman P. Progress in the preclinical discovery and clinical development of class I and dual class I/IV phosphoinositide 3-kinase (PI3K) inhibitors. Curr. Med. Chem. 2011; 18:2686–2714. [PubMed: 21649578]
3. Lu Y, Chen J, Xiao M, Li W, Miller DD. An overview of tubulin inhibitors that interact with the colchicine binding site. Pharm. Res. 2012; 29:2943–2971. [PubMed: 22814904]
4. Ferlin MG, Chiarelotto G, Gasparotto V, Dalla Via L, Pezzi V, Barzon L, Palu G, Castagliuolo I. Synthesis and in vitro and in vivo antitumor activity of 2-phenylpyrroloquinolin-4-ones. J. Med. Chem. 2005; 48:3417–3427. [PubMed: 15857148]
5. Gasparotto V, Castagliuolo I, Chiarelotto G, Pezzi V, Montanaro D, Brun P, Palù G, Viola G, Ferlin MG. Synthesis and biological activity of 7-phenyl-6,9-dihydro-3*H*-pyrrolo[3,2-*f*] quinolin-9-ones: A new class of antimitotic agents devoid of aromatase activity. J. Med. Chem. 2006; 49:1910–1915. [PubMed: 16539377]
6. Ferlin MG, Conconi MT, Urbani L, Oselladore B, Guidolin D, Di Liddo R, Parnigotto PP. Synthesis, in vitro and in vivo preliminary evaluation of anti-angiogenic properties of some pyrroloazaflavones. Bioorg. Med. Chem. 2011; 19:448–457. [PubMed: 21145750]
7. Gasparotto V, Castagliuolo I, Ferlin MG. 3-Substituted 7-phenyl-pyrroloquinolinones show potent cytotoxic activity in human cancer cell lines. J. Med. Chem. 2007; 50:5509–5513. [PubMed: 17915851]

8. Ferlin MG, Bortolozzi R, Brun P, Castagliuolo I, Hamel E, Basso G, Viola G. Synthesis and in vitro evaluation of 3*H*-pyrrolo[3,2-*f*]-quinolin-9-one derivatives that show potent and selective anti-leukemic activity. ChemMedChem. 2010; 5:1373–1385. [PubMed: 20629070]
9. Viola G, Bortolozzi R, Hamel E, Moro S, Brun P, Castagliuolo I, Ferlin MG, Basso G. MG-2477, a new tubulin inhibitor, induces autophagy through inhibition of the Akt/mTOR pathway and delayed apoptosis in A549 cells. Biochem. Pharmacol. 2012; 83:16–26. [PubMed: 21964343]
10. Markman B, Dienstmann R, Tabernero J. Targeting the PI3K/Akt/mTOR pathway–beyond rapalogs. Oncotarget. 2010; 1:530–543. [PubMed: 21317449]
11. Marone R, Cmiljanovic V, Giese B, Wymann MP. Targeting phosphoinositide 3-kinase-moving towards therapy. Biochim. Biophys. Acta, Proteins Proteomics. 2008; 1784:159–185.
12. Goodwin S, Smith AF, Horning EC. Alkaloids of *Lunasia amara blanco*. 4-methoxy-2-phenylquinoline. J. Am. Chem. Soc. 1957; 79:2239–2241.
13. Caddick S, Judd DB, Lewis AKDK, Reich MT, Williams MRV. A generic approach for the catalytic reduction of nitriles. Tetrahedron. 2003; 59:5417–5423.
14. Wu C, Wu F, Bai Y, Yi B, Zhang H. Cobalt boride catalysts for hydrogen generation from alkaline $NaBH_4$ solution. Mater. Lett. 2005; 59:1748–1751.
15. Sahakitpichan P, Ruchirawat S. Highly efficient synthesis of buflavine: A unique Amaryllidaceae alkaloid. Tetrahedron Lett. 2003; 44:5239–5241.
16. van Meerloo J, Kaspers GJ, Cloos J. Cell sensitivity assays: the MTT assay. Methods Mol. Biol. 2011; 731:237–245. [PubMed: 21516412]
17. Lin CM, Ho HH, Pettit GR, Hamel E. Antimitotic natural products combretastatin A-4 and combretastatin A-2: Studies on the mechanism of their inhibition of the binding of colchicine to tubulin. Biochemistry. 1989; 28:6984–6991. [PubMed: 2819042]
18. Hamel E. Evaluation of antimitotic agents by quantitative comparisons of their effects on the polymerization of purified tubulin. Cell Biochem. Biophys. 2003; 38:1–21. [PubMed: 12663938]
19. Bhattacharyya B, Panda D, Gupta S, Banerjee M. Antimitotic activity of colchicine and the structural basis for its interaction with tubulin. Med. Res. Rev. 2008; 28:155–183. [PubMed: 17464966]
20. Verdier-Pinard P, Lai J-Y, Yoo H-D, Yu J, Marquez B, Nagle DG, Nambu M, White JD, Falck JR, Gerwick WH, Day BW, Hamel E. Structure-activity analysis of the interaction of curacin A, the potent colchicine site antimitotic agent, with tubulin and effects of analogs on the growth of MCF-7 breast cancer cells. Mol. Pharmacol. 1998; 53:62–76. [PubMed: 9443933]
21. Berman HM, Westbrook J, Feng Z, Gilliland G, Bhat TN, Weissig H, Shindyalov IN, Bourne PE. The Protein Data Bank. Nucleic Acids Res. 2000; 28:235–242. [PubMed: 10592235]
22. Ravelli RBG, Gigant B, Curmi PA, Jourdain I, Lachkar S, Sobel A, Knossow M. Insight into tubulin regulation from a complex with colchicine and a stathmin-like domain. Nature. 2004; 428:198–202. [PubMed: 15014504]
23. Clarke PR, Allan LA. Cell-cycle control in the face of damage - a matter of life or death. Trends Cell Biol. 2009; 19:89–98. [PubMed: 19168356]
24. Kiyokawa H, Ray D. In vivo roles of CDC25 phosphatases: biological insight into the anti-cancer therapeutic targets. Anti-Cancer Agents Med. Chem. 2008; 8:832–836.
25. Donzelli M, Draetta GF. Regulating mammalian checkpoints through cdc25 inactivation. EMBO Rep. 2003; 4:671–677. [PubMed: 12835754]
26. Ganem NJ, Pellman D. Linking abnormal mitosis to the acquisition of DNA damage. J. Cell Biol. 2012; 199:871–881. [PubMed: 23229895]
27. Orth JD, Loewer A, Lahav G, Mitchison TJ. Prolonged mitotic arrest triggers partial activation of apoptosis, resulting in DNA damage and p53 induction. Mol. Biol. Cell. 2012; 23:567–576. [PubMed: 22171325]
28. Fernandez-Capetillo O, Lee A, Nussenzweig M, Nussenzweig A. H2AX: The histone guardian of the genome. DNA Repair. 2004; 3:959–967. [PubMed: 15279782]
29. García-Sáez AJ. The secrets of the Bcl-2 family. Cell Death Differ. 2012; 19:1733–1740. [PubMed: 22935609]

30. Mollinedo F, Gajate C. Microtubules, microtubule-interfering agents and apoptosis. Apoptosis. 2003; 8:413–450. [PubMed: 12975575]
31. Haldar S, Basu A, Croce CM. Bcl2 is the guardian of microtubule integrity. Cancer Res. 1997; 57:229–233. [PubMed: 9000560]
32. Romagnoli R, Baraldi PG, Brancale A, Ricci A, Hamel E, Bortolozzi R, Basso G, Viola G. Convergent synthesis and biological evaluation of 2-amino-4-(3′,4′,5′-trimethoxyphenyl)-5-aryl thiazoles as microtubule targeting agents. J. Med. Chem. 2011; 54:5144–5153. [PubMed: 21663319]
33. Matson DR, Stukenberg PT. Spindle poisons and cell fate: A tale of two pathways. Mol. Interventions. 2011; 11:141–150.
34. Wertz IE, Kusam S, Lam C, Okamoto T, Sandoval W, Anderson DJ, Helgason E, Ernst JA, Eby M, Liu J, Belmont LD, Kaminker JS, O'Rourke KM, Pujara K, Kohli PB, Johnson AR, Chiu ML, Lill JR, Jackson PK, Fairbrother WJ, Seshagiri S, Ludlam MJC, Leong KG, Dueber EC, Maecker H, Huang DCS, Dixit VM. Sensitivity to antitubulin chemotherapeutics is regulated by MCL1 and FBW7. Nature. 2011; 471:110–114. [PubMed: 21368834]
35. Altieri DC. Survivin and IAP proteins in cell-death mechanisms. Biochem. J. 2010; 430:199–205. [PubMed: 20704571]
36. Castedo M, Perfettini, Roumier T, Andreau K, Medema R, Kroemer G. Cell death by mitotic catastrophe: A molecular definition. Oncogene. 2004; 23:2825–2837. [PubMed: 15077146]
37. O'Connor DS, Grossman D, Plescia J, Li F, Zhang H, Villa A, Tognin S, Marchisio PC, Altieri DC. Regulation of apoptosis at cell division by p34(cdc2) phosphorylation of survivin. Proc. Natl. Acad. Sci. U. S. A. 2000; 97:13103–13107. [PubMed: 11069302]
38. Porcù E, Viola G, Bortolozzi R, Persano L, Mitola S, Ronca R, Presta M, Romagnoli R, Baraldi PG, Basso G. TR-644 a novel potent tubulin binding agent induces impairment of endothelial cells function and inhibits angiogenesis. Angiogenesis. 2013; 16:647–662. [PubMed: 23456551]
39. Profiling Service LeadHunter. KINOMEscan. DiscoveRx; Birmingham, U.K.:
40. Utepbergenov D, Derewenda U, Olekhnovich N, Szukalska G, Banerjee B, Hilinski MK, Lannigan DA, Stukenberg PT, Derewenda ZS. Insights into the inhibition of the p90 ribosomal S6 kinase (RSK) by the flavonol glycoside SL0101 from the 1.5 Å crystal structure of the N-terminal domain of RSK2 with bound inhibitor. Biochemistry. 2012; 51:6499–6510. [PubMed: 22846040]
41. Griffith J, Black J, Faerman C, Swenson L, Wynn M, Lu F, Lippke J, Saxena K. The structural basis for autoinhibition of FLT3 by the juxtamembrane domain. Mol. Cell. 2004; 13:169–178. [PubMed: 14759363]
42. Kulagowski JJ, Blair W, Bull RJ, Chang C, Deshmukh G, Dyke HJ, Eigenbrot C, Ghilardi N, Gibbons P, Harrison TK, Hewitt PR, Liimatta M, Hurley CA, Johnson A, Johnson T, Kenny JR, Bir Kohli P, Maxey RJ, Mendonca R, Mortara K, Murray J, Narukulla R, Shia S, Steffek M, Ubhayakar S, Ultsch M, Van Abbema A, Ward SI, Waszkowycz B, Zak M. Identification of imidazo-pyrrolopyridines as novel and potent JAK1 inhibitors. J. Med. Chem. 2012; 55:5901–5921. [PubMed: 22591402]
43. Chou TC. Theoretical basis, experimental design, and computerized simulation of synergism and antagonism in drug combination studies. Pharmacol. Rev. 2006; 58:621–681. [PubMed: 16968952]
44. Chou TC. Drug combination studies and their synergy quantification using the Chou-Talalay method. Cancer Res. 2010; 70:440–446. [PubMed: 20068163]
45. Bortolozzi R, Viola G, Porcù E, Consolaro F, Marzano C, Pellei M, Gandin V, Basso G. A novel copper(I) complex induces ER-stress-mediated apoptosis and sensitizes B-acute lymphoblastic leukemia cells to chemotherapeutic agents. Oncotarget. 2014; 5:5978–5991. [PubMed: 24980813]
46. Molecular Operating Environment (MOE). Chemical Computing Group Inc.; 1010 Sherbooke St. West, Suite No. 910, Montreal, QC, H3A 2R7, Canada: 2015. version 2014.09
47. Cornell WD, Cieplak P, Bayly CI, Gould IR, Merz KM Jr. Ferguson DM, Spellmeyer DC, Fox T, Caldwell JW, Kollman PA. A second generation force field for the simulation of proteins, nucleic acids, and organic molecules. J. Am. Chem. Soc. 1995; 117:5179–5197.

48. Baxter CA, Murray CW, Clark DE, Westhead DR, Eldridge MD. Flexible docking using Tabu search and an empirical estimate of binding affinity. Proteins: Struct., Funct., Genet. 1998; 33:367–382. [PubMed: 9829696]

49. Halgren TA. Merck molecular force field. I. Basis, form, scope, parameterization, and performance of MMFF94. J. Comput. Chem. 1996; 17:490–519.

50. Stewart, JJP. MOPAC 7. Fujitsu Limited; Tokyo, Japan: 1993.

51. Wojciechowski M, Lesyng B. Generalized Born model: Analysis, refinement, and applications to proteins. J. Phys. Chem. B. 2004; 108:18368–18376.

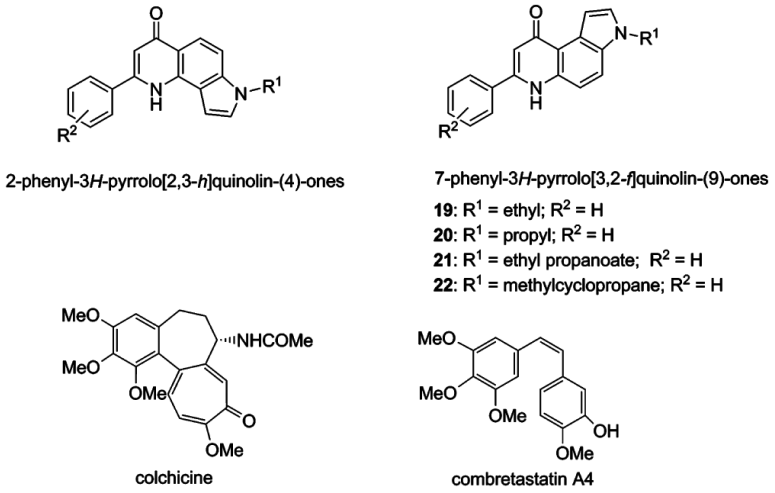

Figure 1.

General chemical structures of 2-PPyQs, 7-PPyQs, the previous 7-PPyQs **19–22**, and the known antitubulin agents colchicine and combretastatin A4.

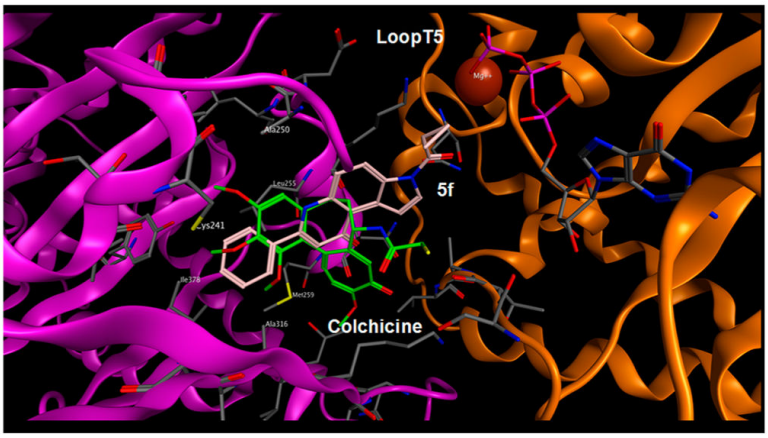

Figure 2.

Comparison of the crystallographic structure of colchicine (in green) in complex with tubulin (Protein Data Bank code 1SA0) and the energetically most favorable pose of **5f** (in pink) obtained by molecular docking simulation. Hydrogen atoms are omitted.

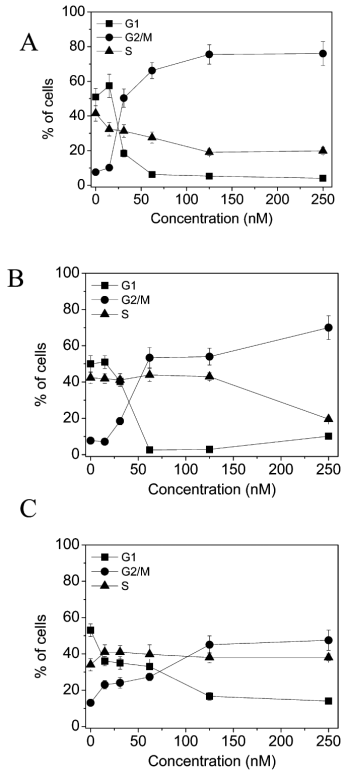

Figure 3.

Percentage of cells in each phase of the cell cycle in HeLa (A), RS4;11 (B), and Jurkat (C) cells treated with **5f** at the indicated concentrations for 24 h. Cells were fixed and labeled with PI and analyzed by flow cytometry as described in the Experimental Section. Data are represented as the mean ± SEM of three independent experiments.

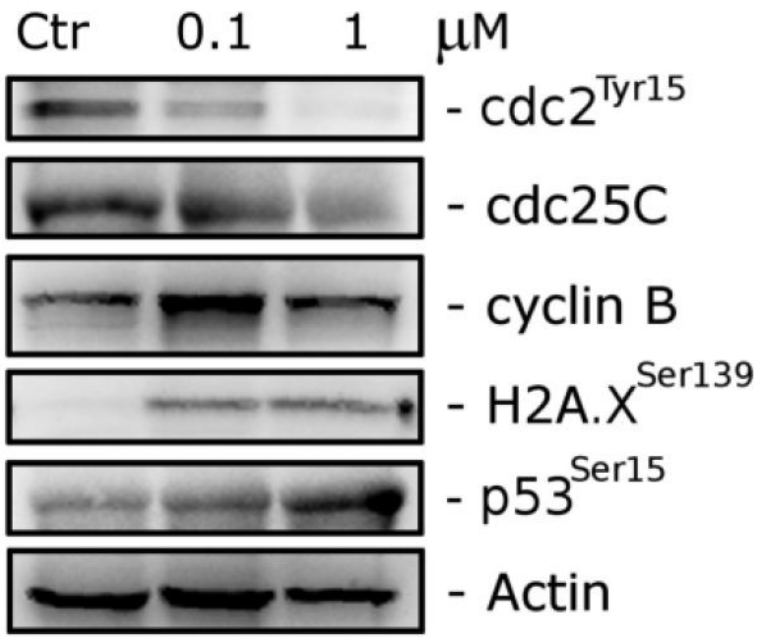

Figure 4.

Effect of **5f** on G2/M regulatory proteins and DNA-damage marker proteins. Jurkat cells were treated for 24 h with the indicated concentration of **5f**. The cells were harvested and lysed for the detection of cyclin B, p-cdc2^{Tyr15}, cdc25C, H2A.X^{Ser139}, and p53^{Ser15} expression by Western blot analysis. To confirm equal protein loading, each membrane was stripped and reprobed with an anti-β-actin antibody.

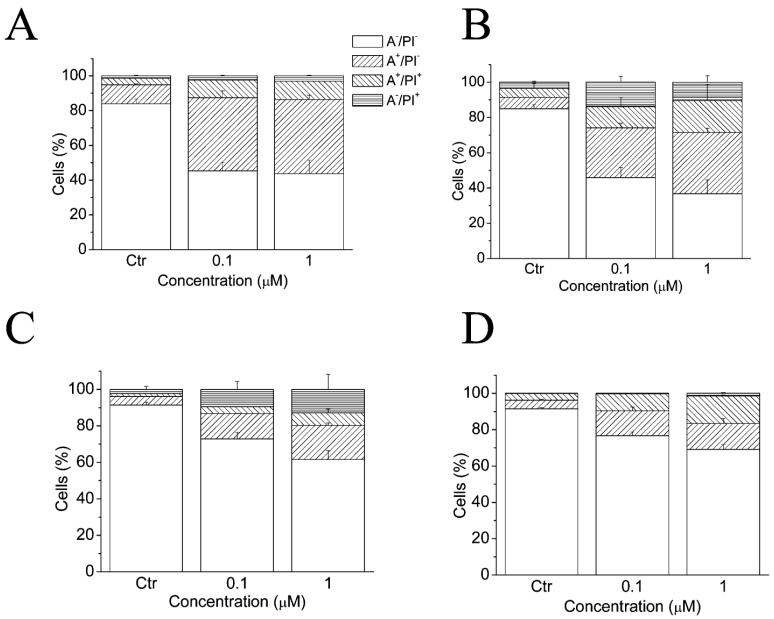

Figure 5.

Flow cytometric analysis of apoptotic cells after treatment of HeLa (A), Jurkat (B), RS4;11 (C), and K562 (D) cells with **5f** at the indicated concentrations after incubation for 24 h. The cells were harvested and labeled with annexin-V-FITC and PI and analyzed by flow cytometry. Data are represented as the mean ± SEM of three independent experiments.

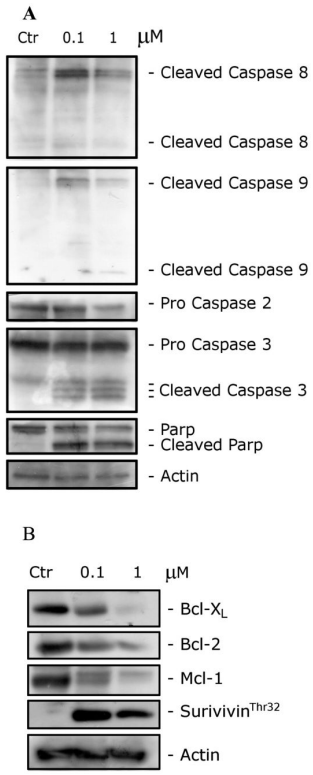

Figure 6.

(A). Western blot analysis of caspase-8, caspase-9, caspase-2, caspase-3, and PARP after a 24 h treatment of Jurkat cells with **5f** at the indicated concentrations. (B) Western blot analysis of Bcl-XL, Bcl-2, survivin^{Thr32}, and Mcl-1 after treatment of Jurkat cells with **5f** at the indicated concentrations for 24 h. To confirm equal protein loading, each membrane was stripped and reprobed with an anti-β-actin antibody.

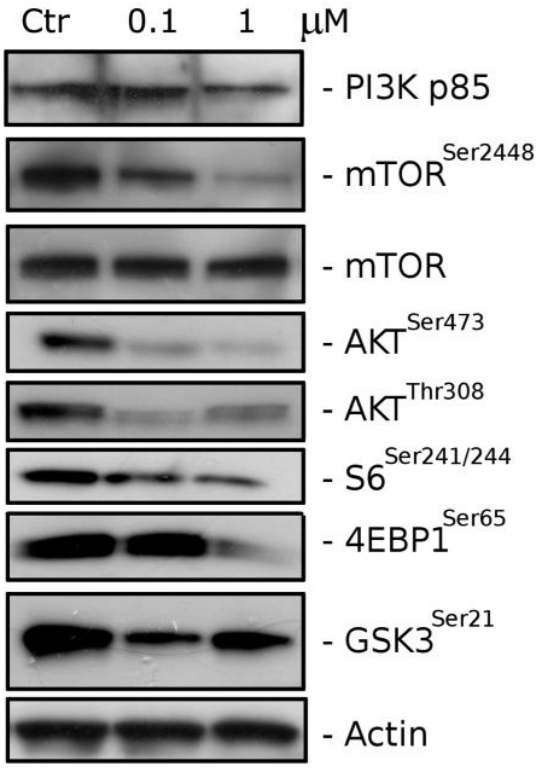

Figure 7.

Western blot analysis of PI3K/AKT/mTOR after treatment of Jurkat cells with **5f** at the indicated concentrations for 24 h. To confirm equal protein loading, each membrane was stripped and reprobed with an anti-*β*-actin antibody.

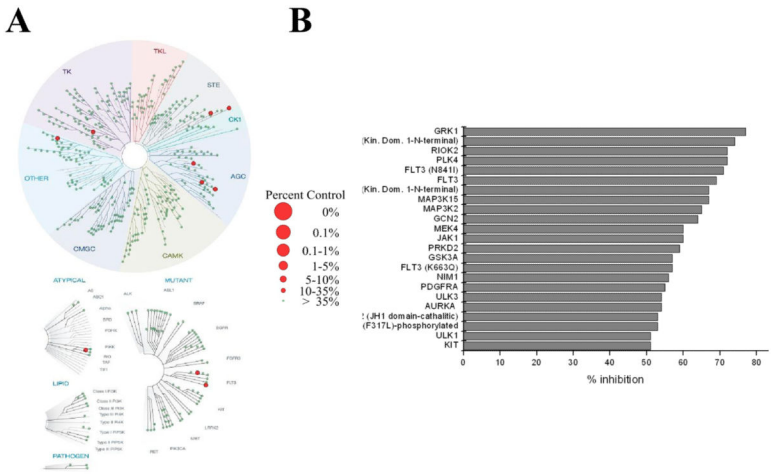

Figure 8.

(A) TREEspot interaction maps: kinases found to bind **5f** are marked with red circles, where larger circles indicate higher affinity binding and the side percentages indicate residual kinase activity. (B) Histogram of the inhibitory activity of **5f** on kinases inhibited more than 50%.

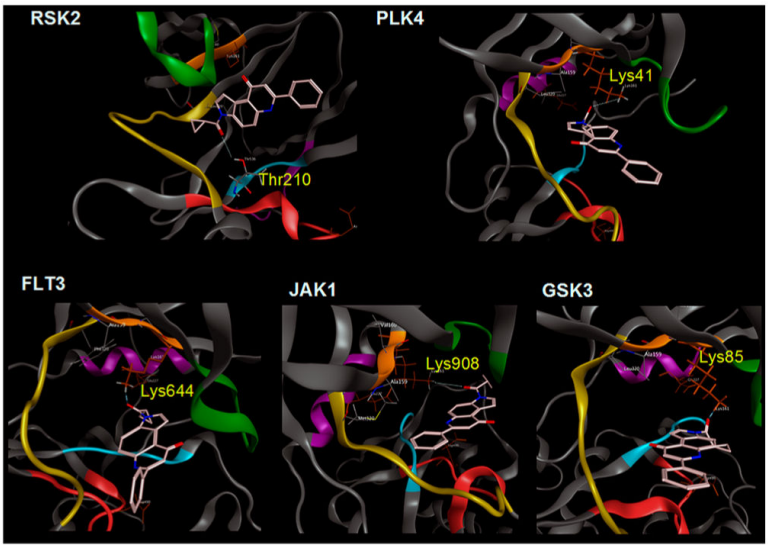

Figure 9.

Energetically most favorable pose of **5f** (in pink) in the ATP binding side of selected protein kinases.

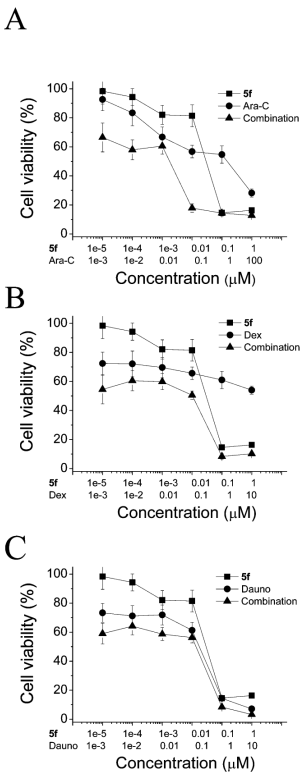

Figure 10.

Effect of **5f** treatment alone and in combination with difierent chemotherapic drugs in MV4;11 cells. Cells were treated at the indicated concentrations and at a fixed combination ratio, and viability was assessed by the MTT test after a 48 h incubation. Data are expressed as the mean ± SEM of three independent experiments.

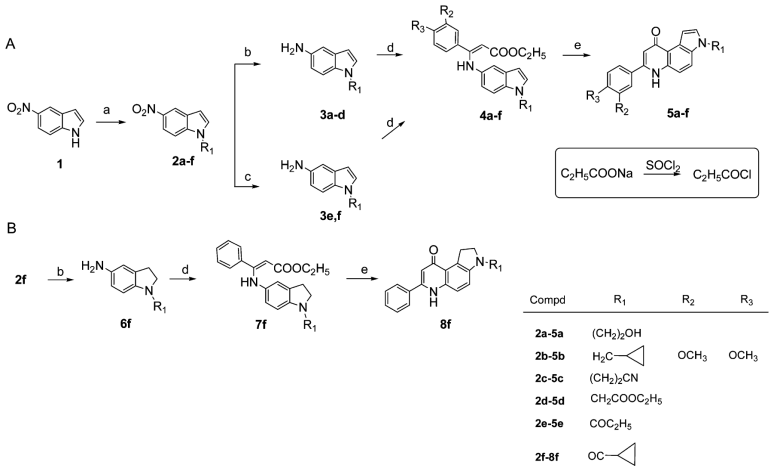

Scheme 1. Synthetic Routes to PPyQs 5a–f (A) and 8f (B)[a]

[a]Reagents and conditions: (a) NaH 60%, bromoethyl alcohol, cyclopropylmethyl bromide, 3-bromopropionitrile, ethyl chloroacetate, cyclopropylcarbonyl chloride, *n*-propionyl chloride, anhydrous DMF, rt, 3 h, 47–99%; (b) H_2, Pd/C 10%, ethyl acetate, 50 °C, 4–14 h, 90–98%; (c) $SnCl_2$/HCl, CH_3OH, reflux, 1.5 h, 47–80%; (d) ethyl benzoylacetate or ethyl dimethoxybenzoylacetate, absolute ethanol, reflux 15 h, 37–87%; (e) diphenyl ether, 250 °C, 10–15 min, 30–76%.

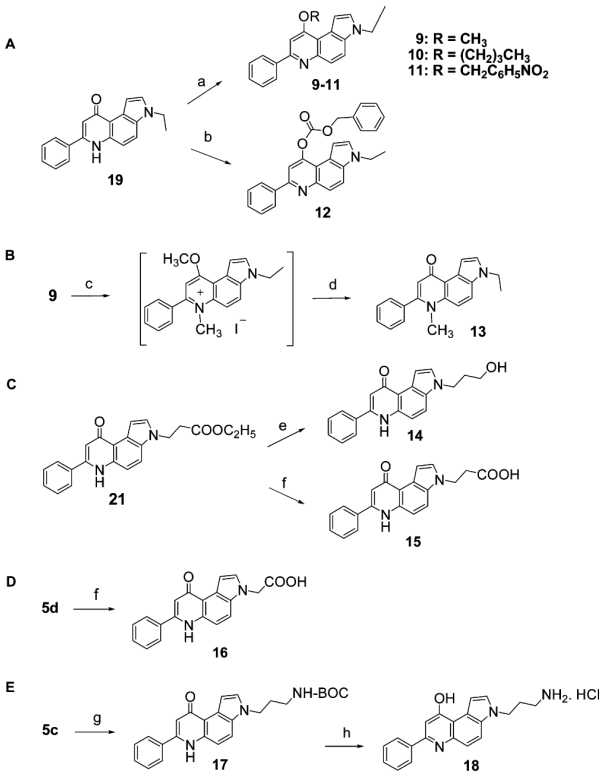

Scheme 2. Synthesis of 7-PPyQs 9–18[a]

[a] Reagents and conditions: (a) CH_3 I or $Br(CH_2)_3CH_3$, $BrCH_2C_6H_5NO_2$, NaH, DMF, rt, 2 h, 64–74%; (b) $C_6H_5CH_2OCOCl$, NaH, DMF, 0 °C, 2 h, 96%; (c) CH_3I, reflux; (d) NaOH 1 N, reflux, 18%; (e) $LiAlH_4$, anhydrous THF, rt, 3 h, 70%; (f) NaOH 1 N, methanol, reflux, 2 h, 85%; (g) $NaBH_4$, $CoCl_2 \cdot 6H_2O$, di-*tert*-butyl dicarbonate, methanol, 10 h, 77%; (h) HCl dry gas, ethyl acetate, 58%.

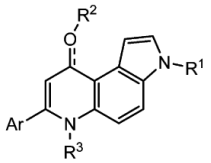

Subset 1: R^3= H, Ar= phenyl

R^1 = **19** CH_2-CH_3
5a CH_2-CH_2-OH
5d CH_2COOCH_2-CH_3
16 CH_2-COOH

Subset 2: R^3= H, Ar= phenyl

R^1 = **20** CH_2-CH_2-CH_3
5c CH_2-CH_2-C N
14 CH_2-CH_2-CH_2-OH
15 CH_2-CH_2-COOH
18 CH_2-CH_2-CH_2-NH_2
21 CH_2-CH_2-$COOCH_2$-CH_3

Subset 3: R^3= H, Ar= phenyl

R^1 = **20** CH_2-CH_2-CH_3
5e CO-CH_2-CH_3
22 CH_2 -cyclopropane
5f CO-cyclopropane

Subset 4: R^1= CH_2-CH_3, Ar= phenyl

R^2 = **9** CH_3
10 $(CH_2)_3$-CH_3
11 benzyl
12 $COOCH_2$Ph

R^1= CH_2-CH_3, Ar= phenyl
R^3 = **13** CH_3

R^1= CH_2-CH_3, R_3 =H
Ar = **5b** 3,4-dimethoxyphenyl

Scheme 3. Subsets of 7-PPyQ Derivatives Prearranged for the Structure–Antiproliferative Activity Relationships Discussion

Table 1

Growth Inhibitory Activity of PPyQ derivatives 5a–f, 8f, 9–16, and 18–22 for Human Cancer Solid Tumor (A) and Leukemic Cell Lines (B)

	(A) GI_{50} (nM)[a]				
compd	HeLa	A549	HT-29	MCF-7	OVCAR-3
5a	1563 ± 135	7756 ± 1126	236 ± 16	256 ± 31	9863 ± 1236
5b	2856 ± 736	7456 ± 3601	>10000	>10000	>10000
5c	191 ± 72	928 ± 125	356 ± 61	82 ± 21	326 ± 17
5d	2456 ± 231	4785 ± 432	34589 ± 119	2863 ± 61	>10000
5e	5 ± 2	78 ± 4	12 ± 8	3 ± 1	12 ± 5
5f	1 ± 0.6	9 ± 0.4	1 ± 0.5	5 ± 1	71 ± 12
8f	38 ± 0.5	145 ± 78	15 ± 8	19 ± 8	243 ± 51
9	111 ± 51	45 ± 9	1456 ± 623	1863 ± 921	32 ± 9
10	>10000	>10000	>10000	>10000	>10000
11	>10000	>10000	>10000	>10000	>10000
12	15 ± 1	21 ± 5	18 ± 8	211 ± 20	9 ± 2
13	936 ± 41	463 ± 65	923 ± 221	1656 ± 632	1236 ± 258
14	175 ± 12	311 ± 125	48 ± 7	95 ± 16	38 ± 8
15	5563 ± 55	>10000	>10000	>10000	>10000
16	>10000	>10000	>10000	>10000	>10000
18	551 ± 5	1072 ± 119	1569 ± 62	389 ± 112	2136 ± 369
19 [b]	11 ± 8	32 ± 15	32 ± 12	45 ± 11	32 ± 11
20 [b]	2 ± 0.9	nd	5±1	2 ± 1	nd
21 [c]	452 ± 102	nd	492 ± 85	589 ± 189	nd
22 [b]	21 ± 12	21 ± 2	61 ± 1	42 ± 15	14 ± 8

	(B) GI_{50} (nM)[a]								
compd	MOLT-3	CCRF-CEM	HL-60	K562	RS4;11	Jurkat	SEM	MV4;11	THP-1
5a	252 ± 53	4705 ± 2122	254 ± 11	9±1	74 ± 32	845 ± 19	161 ± 33	311 ± 42	2850 ± 918
5b	5850 ± 2301	>10000	1324 ± 351	6936 ± 432	275 ± 171	2450 ± 323	452 ± 61	1986 ± 232	4632 ± 126
5c	131 ± 33	392 ± 161	274 ± 42	nd	83 ± 42	1905 ± 832	92 ± 12	323 ± 6	49 ± 9
5d	201 ± 67	>10000	2415 ± 152	5213 ± 1265	263 ± 105	2211 ± 453	1650 ± 221	2305 ± 1123	>10000
5e	5.1 ± 1.3	2.1 ± 0.9	2.5 ± 0.5	nd	1 ± 0.5	0.4 ± 0.2	9 ± 2	36 ± 2	125 ± 32
5f	2.3 ± 1.4	17 ± 4	2.0 ± 0.6	6 ± 2	0.1 ± 0.05	0.3 ± 0.03	0.4 ± 0.1	19 ± 8	74 ± 25
8f	145 ± 52	232 ± 35	172 ± 5	82 ± 10	5 ± 1	14 ± 3	19 ± 2	513 ± 112	355 ± 72
9	163 ± 44	115 ± 42	27 ± 3	21 ± 9	3 ± 0.1	18 ± 2	23 ± 6	37 ± 13	34 ± 12
10	>10000	>10000	>10000	>10000	>10000	>10000	>10000	>10000	>10000
11	>10000	>10000	>10000	>10000	>10000	>10000	>10000	>10000	>10000
12	8.5 ± 3.2	18 ± 5	3 ± 0.5	3 ± 0.8	0.5 ± 0.2	0.4 ± 0.06	1 ± 0.1	4 ± 0.8	1 ± 0.6
13	145 ± 21.2	526 ± 123	145 ± 21	1142 ± 532	231 ± 61	30 ± 2	623 ± 212	1569 ± 521	821 ± 236

14	21.5 ± 11.6	405 ± 78	29 ± 6	78 ± 12	8 ± 2	8 ± 3	14 ± 3	78 ± 12	408 ± 51
15	>10000	>10000	>10000	>10000	>10000	>10000	>10000	>10000	>10000
16	>10000	>10000	2375 ± 372	>10000	7756 ± 1231	>10000	>10000	>10000	>10000
18	515 ± 45	2423 ± 581	951 ± 51	nd	82 ± 11	482 ± 75	158 ± 51	492 ± 35	271 ± 18
19	nd	nd	0.5 ± 0.02	1 ± 0.1	2 ± 0.3	0.5 ± 0.2	nd	nd	nd
20	nd	nd	nd	nd	0.6 ± 0.4	0.9 ± 0.3	nd	nd	nd
21	nd	nd	2.0 ± 0.1	196 ± 61	2 ± 0.4	0.5 ± 0.01	nd	nd	nd
22	nd	nd	6.1 ± 0. 5	1 ± 0.4	2 ± 0.5	0.5 ± 0.03	nd	nd	nd

[a] GI_{50}= compound concentration required to inhibit tumor cell proliferation by 50%. Data are presented as the mean ± SEM from the dose–response curves of at least three independent experiments. nd not determined.

[b] Referencef 7.

[c] Reference 8.

Table 2

Cytotoxicity of 5f in Human Noncancer Cells

	GI_{50} (μM)[a]	
cell line	**5f**	**22**
$PBL_{resting}$[b]	>100	77.6 ± 20.0
PBL_{PHA}[c]	95.7 ± 8.9	5.0 ± 0.9
HUVEC	22.1±10.9	7.8 ± 0.55

[a] Compound concentration required to reduce cell growth by 50%. Values are the mean ± SEM for three separate experiments.

[b] PBL not stimulated with PHA.

[c] PBL stimulated with PHA.

Table 3

Inhibition of Tubulin Polymerization and Colchicine Binding by Compounds 5a–f, 8f, 9, 12–22, and CA–4

compd	inhibition of tubulin assembly IC_{50} ± SD (μM)[a,c]	inhibition of colchicine binding inhibition ± SD (%)[b,c]
5a	2.9 ± 0.1	11 ± 4
5b	>20	nd
5c	1.3 ± 0.05	20 ± 1
5d	6.6 ± 0.3	nd
5e	0.99 ± 0.1	52 ± 5
5f	0.99 ± 0.1	69 ± 3
8f	2.6 ± 0.2	30 ± 4
9	5.7 ± 0.7	nd
12	0.74 ± 0.07	77 ± 2
13	1.8 ± 0.3	61 ± 1
14	1.2 ± 0.1	40 ± 0.9
15	8.0 ± 0.1	nd
16	>20	nd
18	>20	nd
19 [d]	0.57 ± 0.02	73 ± 0.7
20 [d]	0.58 ± 0.05	77 ± 3
21 [e]	0.75 ± 0.04	75 ± 4
22 [d]	0.90 ± 003	83 ± 0.5
CA-4	1.2 ± 0.1	99 ± 0.06

[a] Inhibition of tubulin polymerization. Tubulin was at 10 μM.

[b] Inhibition of [^{3}H]colchicine binding.

[c] Tubulin and colchicine were at 1 and 5 μM, respectively, and the tested compounds were at 5 μM. nd, not determined.

[d] Reference 7.

[e] Reference 8.

Table 4

Relevant Binding Features of 5f against Five Selected Protein Kinases

protein kinase	crucial H-bonding interaction with amide moiety in 3-position of 5f	$\Delta(\Delta E_{inter})_{IV\rightarrow 5f}$ [a] (kcal/mol)
RSK2	Thr210 ($d_{C=O/HO} \approx 2.8$ Å)	−6.5
PLK4	Lys41 ($d_{C=O/HN} \approx 3.1$ Å)	−4.5
FLT3	Lys644 ($d_{C=O/hn} \approx 2.1$ Å)	−9.0
JAK1	Lys908 ($d_{C=O/HN} \approx 3.0$ Å)	−5.0
GSK3	Lys85 ($d_{C=O/HN} \approx 2.2$ Å)	−6.0

[a] $\Delta(\Delta E_{inter})_{IV\rightarrow 5f} = [(\Delta E_{inter})_{IV}] - [(\Delta E_{inter})_{5f}]$.

Table 5

Compound 5f Synergizes with Drugs Used in Leukemia Therapy

CI[a]	Dex + 5f (10:1)[b]	Dauno + 5f (10:1)[b]	AraC + 5f (100:1)[b]
		Jurkat Cell Line	
CI (GI_{50})	0.67	0.21	11.9
CI (GI_{75})	0.81	0.45	0.79
CI (GI_{90})	0.97	1.0	14.7
		MV4;11 Cell Line	
CI (GI_{50})	0.016	0.22	0.09
CI (GI_{75})	0.06	0.17	0.38
CI (GI_{90})	0.25	0.14	1.8
		THP-1 Cell Line	
CI (GI_{50})	0.22	0.17	0.14
CI (GI_{75})	0.17	0.17	0.15
CI (GI_{90})	0.13	0.17	0.15

[a] Combination indexes evaluated at different points.

[b] Molar combination ratios.